

HELSINKI INSTITUTE OF PHYSICS
INTERNAL REPORT SERIES
HIP – 2007 – 03

COMPUTATIONAL MODELLING OF LIPID BILAYERS WITH SPHINGOMYELIN AND STEROLS

PERTTU NIEMELÄ

Laboratory of Physics and Helsinki Institute of Physics,
Helsinki University of Technology
Espoo, Finland

Academic Dissertation

Dissertation for the degree of Doctor of Science in Technology to be presented with due permission of the Department of Engineering Physics and Mathematics for public examination and debate in Auditorium E at Helsinki University of Technology (Espoo, Finland) on the 20th of June, 2007, at 12 o'clock noon.

ISBN 978-952-10-3712-2 (print)
ISBN 978-952-10-3713-9 (electronic)
ISSN 1455-0563
URL <http://lib.tkk.fi/Diss/list.html#2007>

Abstract

This thesis is based on atom-scale molecular dynamics simulations on lipid bilayers. The study concentrates on structural and dynamic properties of lipid bilayers, involving three lipid classes that are the main constituents of, for example, eukaryotic plasma membranes: phosphatidylcholines (PCs), sphingomyelins (SMs) and sterols. The discussion in the thesis starts from the simplest bilayers that are comprised of single lipid components, and gradually moves towards more complex systems, approaching a better description of biological membranes.

Studies on single-component bilayers concentrate on the properties of SM. In a comparison with a structurally similar PC, it is shown that the packing of SM in a bilayer is more compact and that the lipids are more ordered than in a PC bilayer. Additionally, unsaturation increases the fluidity of SM bilayer less than typically in PC bilayers. The above differences in the bilayer properties of SM and PC are explained by detailed analysis of the intra- and intermolecular hydrogen bonding in the SM bilayer. The results on the effects of chain length on SM bilayers are mainly involved with the bilayer thickness and the interdigitation of the longer chains through the bilayer centre.

The studies on sterols involves two parts. First, the molecular interactions of cholesterol (CHOL) with PC and SM lipids are characterised in detail. In particular, the aim is to reveal aspects of the SM-CHOL interaction, which has been proposed to be a key factor in the formation of lateral domains called lipid rafts in biological membranes. Second, the properties of bilayers with binary mixtures of PC and different sterols are discussed. It is shown that the acyl chain order in the studied systems is correlated with the tilt of

the sterol. Also, we find that CHOL is superior among the studied sterols in ordering the acyl chains.

The studies on lipid raft bilayers involve three component mixtures of PC, SM, and CHOL. Large-scale simulations of two types of lipid environments are compared: raft-like membranes, which are high in SM and CHOL concentration, and non-raft membranes, which comprise of mostly PC. The results reveal that the raft-like membranes are much more rigid, ordered and packed, but also characterised by slower dynamics of the lipids, when compared to the non-raft environment. In the discussion, we show that the different properties of the two membrane environments may have significant implications on the functioning and partitioning of membrane proteins. In particular, the observed differences in the lateral pressure profiles are suggested to alter the open-state probability of an ion channel MscL.

Preface

The work reported in this thesis has been done in the Laboratory of Physics and Helsinki Institute of Physics at Helsinki University of Technology during 2003-2007. I would like to thank the supervisor of this thesis, professor Risto Nieminen. He has created an excellent, creative, international, and well-functioning working atmosphere at COMP.

My deepest gratitude goes to professor Ilpo Vattulainen and Dr. Marja Hyvönen, who have guided me through this thesis project and who have probably the biggest influence on the results presented in this thesis. Ilpo has not only taught me how to do great science, but also set an example of an enthusiastic, hard-working and successful scientist, who manages to be laid-back at the same time. Ilpo also really takes care of the well-being of his students. Marja is an endless resource of excellent, biologically relevant research ideas and she is always keen to discuss even the minor practical details of research.

I thank the pre-examiners of this thesis, professor J. Peter Slotte and professor Erik Lindahl for providing a number of excellent comments and insights. Also, I am thankful to Ilpo, Marja, Samuli, Jussi, and Tomek for proofreading the manuscript.

A number of other people have influenced the results in this thesis. First, I wish to thank all co-authors of the publications. Jussi showed astonishing creativity and persistence in analysing the simulation data, which is greatly appreciated. Discussions with Samuli have clarified many things, as he makes an accurate analysis of just about any physical quantity. Tomek is a real expert, both on simulation methods and on virtually any possible

lipid system. I have never met professor Pasenkiewicz-Gierula, but it is an honour to have a joint publication with her. I am thankful to Mikko Karttunen for providing new innovative ideas, but also for excellent lectures and exercises, which are hard work but very educative.

During this time in Espoo I have had the chance to work with a group of colleagues, who have created a most enjoyable atmosphere. Special thanks to my room mates Andrey and Markus, with whom we have had long and numerous discussions about science, life, and anything possible. Thanks also to other members of our young and dynamic group: Anette, Artturi, Andrea, Emma F, Emma T, Emppu, Jarmila, Katariina, Kimmo, Koos, Lei, Lorna, Michael, Mikko H, Mikko K, Olli, Teemu, Timo, Sanja, Wei, and everyone else. I am grateful to professor Peter Tieleman for a change to visit his group. The six months in Calgary taught me a great deal about proteins and force fields. Thanks to the fun bunch of people there: Anirban, Ben, Carolyn, Christian, Eliud, Jirasak, Justin, Leilia, Luca, Marian, Mark, Megan, Ryan, Svetlana, and Walter.

Friends have made an important contribution to the thesis by giving a reason to do other things besides research. Thanks to Tero & Sanna, Apeli, Jussi, Oltso, Teemu & Jenni, Pii & Tuukka, Jonna, Mari, Meri, Miika & Salla, Lauri & Katri, Juhis & Diep, Timo & Katja, Antti & Riikka, and all others. Without you there would be no thesis.

Financial support from Finnish Academy of Science and Letters and the Academy of Finland are acknowledged. I would also like to thank the computing resources provided by the Finnish IT Center for Science and the HorseShoe supercluster at the University of Southern Denmark.

I am grateful to my parents Pentti and Maija-Liisa, for their endless support and encouragement. My warmest thanks to Jenni and Markku, as well as Riitta, Petteri & Liisa, who are always helpful when needed. Above all, I thank my dear wife Emma, who has been most supporting, understanding, and loving during the years of thesis writing.

Espoo, May 2007

Perttu Niemelä

Contents

Abstract	iii
Preface	v
List of Publications	ix
Overview	xi
1 Background	1
1.1 Overview of Biological Membranes	1
1.2 About Lipid Molecules	3
1.3 Phase Behaviour of Lipids	8
2 Research Method	15
2.1 Classical Molecular Dynamics	15
2.2 Simulation vs. Experiment	30
2.3 Systems Studied in This Work	35
3 Properties of Sphingomyelin	37
3.1 Motivation	37
3.2 Comparison of PSM with DPPC	37
3.3 Hydrogen Bonding	39
3.4 Effects of Chain Length and Saturation	41
3.5 Interdigitation	43

4	Properties of Sterols	45
4.1	Motivation	45
4.2	Ordering Capacity of Cholesterol	46
4.3	Direct Hydrogen Bonding	48
4.4	Head Group Interactions	49
4.5	Sterol Tilt vs. Fluidity	51
4.6	Comparison of Sterols	52
5	Lipid Raft Simulations	55
5.1	Motivation	55
5.2	Overview of Membrane Properties	56
5.3	Undulations and Bending Rigidity	57
5.4	Area Compressibility	61
5.5	Lateral Heterogeneity	61
5.6	Lateral Pressure Profiles	63
5.7	Effects on Membrane Proteins	64
6	Summary	67
	Bibliography	69

List of Publications

This thesis consists of an introduction and the following publications:

- I Niemelä, P., Hyvönen, M.T., and Vattulainen, I., *Structure and Dynamics of Sphingomyelin Bilayer: Insight Gained Through Systematic Comparison to Phosphatidylcholine*, Biophysical Journal **87**, 2976–2989 (2004),
- II Niemelä, P., Hyvönen, M. T., and Vattulainen, I., *Influence of Chain Length and Unsaturation on Sphingomyelin Bilayers*, Biophysical Journal **90**, 851–863 (2006),
- III Aittoniemi, J., Róg, T., Niemelä, P., Pasenkiewicz-Gierula, M., Karttunen, M., and Vattulainen, I., *Tilt: Major Factor in Sterols' Ordering Capability in Membranes*, Journal of Physical Chemistry B **110**, 25562–25564 (2006),
- IV Aittoniemi, J., Niemelä, P. S., Hyvönen, M. T., Karttunen, M., and Vattulainen, I., *Insight into the Putative Specific Interactions between Cholesterol, Sphingomyelin and Palmitoyl-Oleoyl Phosphatidylcholine*, Biophysical Journal **92**, 1125–1137 (2007), and
- V Niemelä, P. S., Ollila, S., Hyvönen, M. T., Karttunen, M., and Vattulainen, I., *Assessing the Nature of Lipid Rafts*, PLoS Computational Biology **3**, e34 (2007).

The author has played an active role in all stages of the research reported in this thesis.

Publications I and II were authored together with Marja Hyvönen and Ilpo Vattulainen. The author participated actively in the planning of the simulations and in developing the force field parameters. The author carried out the simulations, wrote the analysis codes and conducted the analysis. The author also wrote the first draft of the publications.

Publication III was done together with Jussi Aittoniemi, Tomasz Róg, Martha Pasenkiewicz-Gierula, Mikko Karttunen, and Ilpo Vattulainen. In this project, the author participated in planning the analysis and writing the publication. The simulations were carried out by Tomasz Róg and the analysis was done by Jussi Aittoniemi. The author co-supervised the work done by Jussi Aittoniemi. The first draft of the publication was written by Jussi Aittoniemi.

Publication IV was co-authored with Jussi Aittoniemi, Marja Hyvönen, Mikko Karttunen and Ilpo Vattulainen. The author participated actively in planning the simulations and carried out the simulations. Also, the author had an active role in planning the analysis, which was mainly carried out by Jussi Aittoniemi. The author co-supervised the work done by Jussi Aittoniemi. The first draft of the publication was written by Jussi Aittoniemi.

Publication V was co-authored with Samuli Ollila, Marja Hyvönen, Mikko Karttunen and Ilpo Vattulainen. The author participated in planning the simulations and analysis. The author executed the simulations and conducted most of the analysis, except for the lateral pressure profiles, which were calculated by Samuli Ollila. The first draft of the publication was written by the author.

Overview

This thesis is about computational modelling of lipid bilayers, concentrating on such lipid compositions that are interesting from a biological point of view. Here, the structure of the thesis is outlined.

In Chapter 1, an introduction to biological membranes and biologically relevant lipids is written on the basis of literature review. In Chapter 2, the research method used in this study is introduced, including a discussion on the utilised force field parameters and the main limitations involved with the method. In addition, the main features of the utilised analysis methods are reviewed together with aspects on how to relate the results from simulation systems with experiments.

The most important results are summarised in Chapters 3 to 5, which are divided in the following way. Chapter 3 is based on *Paper I* and *Paper II* and it discusses the main results for single-component bilayers involving sphingomyelin, comparing them with phosphatidylcholines. In contrast, Chapter 4 is based on *Paper III* and *Paper IV*, and it concentrates on the effects of cholesterol and other sterols on the properties of lipid bilayers. In particular, the nature of the local molecular interactions of cholesterol with other membrane lipids are discussed. Chapter 5 is based on *Paper V*, and it discusses the properties of lipid bilayers that have high concentrations of both sphingomyelin and cholesterol and compares the large-scale properties of these bilayers with more fluid bilayers.

Background

1.1 Overview of Biological Membranes

The first cell probably came into being when a membrane formed, enclosing a small volume of aqueous solution and separating it from the rest of the universe [Nelson and Cox, 2005]. It is difficult to overestimate the importance of membranes for life, considering that they surround all cells and control everything that goes in or out of the cell. In addition to the plasma membrane, there is a significant number of membranes within the cell, surrounding several organelles, compartments, and the nucleus of eukaryotic cells. Most of the intracellular processes take place within or at these membranes [Purves et al., 2004].

Typically, membranes consist of lipids, proteins and carbohydrates. The backbone of any membrane is formed by the lipid bilayer, which is a few nanometres in thickness. The classical picture of a lipid bilayer is the one of a flexible, two dimensional fluid, whose primary function is to act as a passive diffusion barrier for various substances and to provide a platform for membrane proteins to attach [Singer and Nicolson, 1972]. In recent years, however, this picture has been updated, highlighting the role of the *dynamic structure* in lipid bilayers and the possibility that the lipids themselves play an active role in regulating a number of cellular processes, for example through affecting the activity of membrane proteins [Simons and Ikonen, 1997].

The mass fraction of proteins in membranes ranges from about 0.30 to 0.75, but as proteins are much larger than lipids, they are by far outnumbered by lipids [Nelson and Cox, 2005]. For example, proteins are responsible for the active transport of substances across the membrane and about various other processes. They attach to the lipid bilayer either by specific anchors, or by spanning their hydrophobic parts across the bilayer. Carbohydrates, which are attached to lipids and proteins, form the glycocalyx network on the extracellular side of the plasma membrane, typically increasing the effective thickness of the membrane up to 50 nm [Sackmann, 1995]. The glycocalyx is important for communication between the cell and its environment, but also for connecting the cell with the extracellular matrix.

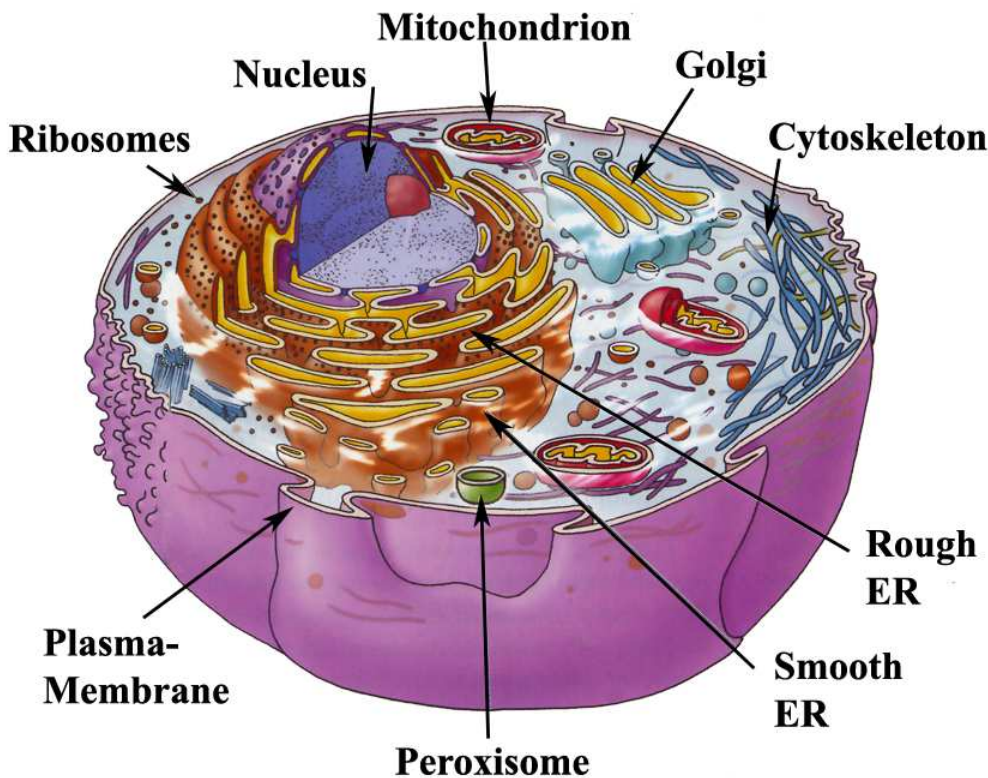


Figure 1.1: A cartoon showing the structure of an eukaryotic cell. Figure adapted from [Purves et al., 2004].

Figure 1.1 shows a drawing of the interior of an eukaryotic cell, including the most important organelles. The nucleus serves as a container for most of the genetic material. The construction of proteins takes place within

the rough endoplasmic reticulum (ER), and further modifications are done in the smooth ER and Golgi apparatus. For example, at the smooth ER carbohydrates are added to the proteins. Finally, either small targeting sequences or the carbohydrates added to the protein are used as addresses in order to deliver the proteins to their destinations.

Lipids are mostly synthesised in the smooth endoplasmic reticulum. For example, cholesterol and ceramide (a precursor of sphingomyelin) are synthesised in the smooth ER [Simons and Ikonen, 2000]. From there, ceramide is transferred to the Golgi by a transfer protein CERT [Hanada, 2006] and finally, a PC headgroup is added to form sphingomyelin [Ohanian and Ohanian, 2001]. Once complete, the lipids are then transferred to their destinations by vesicles and/or transfer proteins.

1.2 About Lipid Molecules

1.2.1 Lipid Composition of Membranes

The number of lipid species in biomembranes is astonishingly large, over 1000 in total [van Meer, 2005]. For example, in erythrocytes alone this number is about 100 [Sackmann, 1995]. One major question in membrane research is to explain this variety: whether it is a left-over of evolution or whether all lipid species are really needed.

One definition for lipids (by W. W. Christie) is that they are fatty acids and their derivatives, and substances related biosynthetically or functionally to these compounds. Lipids can be divided into three classes on the basis of their function: storage lipids such as fats, structural lipids of membranes, and signalling lipids [Nelson and Cox, 2005]. Figure 1.2 shows examples of structural lipids of biological membranes, which are the subject of this thesis.

In phospholipids, the glycerol backbone facilitates a high variability of different headgroups and acyl chain combinations. The main headgroup classes are the phosphatidylcholine (PC), phosphatidylethanolamine (PE), phosphatidylserine (PS) and phosphatidylinositol (PI), of which the two latter are charged [Sackmann, 1995]. The acyl chains typically vary between 16 and 22 carbons in length and they contain 0 to 6 double bonds. Figure 1.2A shows a typical phospholipid, the palmitoyl-oleoyl-PC (POPC), which contains the PC-headgroup and two different, ester bonded acyl chains: palmitoyl and oleoyl.

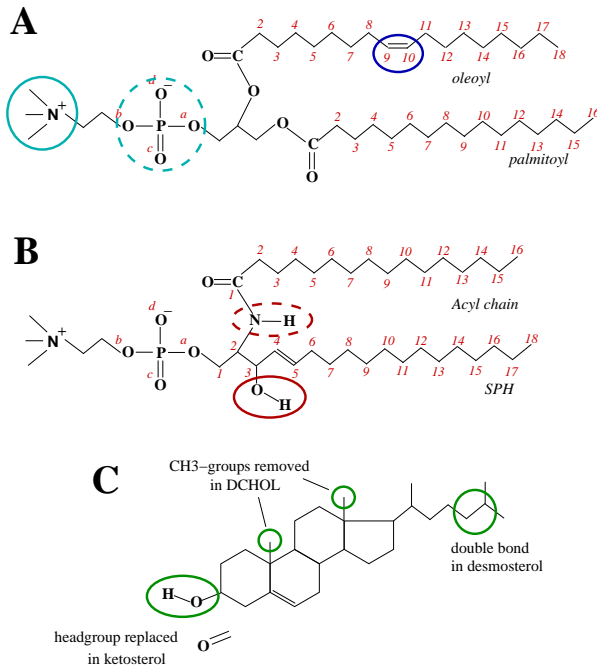


Figure 1.2: Molecular structure of three membrane lipids: A) POPC, B) PSM, and C) CHOL. The important functional groups have been indicated with different colours: the phosphate (cyan, dashed) and choline (cyan) of the PC-headgroup, together with the *cis*-double bond (blue) of the monounsaturated chain. The two hydrogen donor groups of SM are the amide group (red dashed) and the hydroxyl group (red). For CHOL, three modifications studied in this work are indicated.

Typical sphingolipids have either the PC-headgroup (sphingomyelin, SM) or a sugar residue (glycosphingolipids) [Nelson and Cox, 2005]. For SM, the headgroup structure and the length of the sphingosine (SPH) chain are usually fixed, but the length and saturation of the amide-linked acyl chain can vary. The acyl chains of SMs are typically very long (up to 24-26 carbons) and highly saturated [Ramstedt and Slotte, 2002]. Figure 1.2B shows the structure of a palmitoyl-SM (PSM).

The molecular structure of sterols is characterised by the rigid and hydrophobic ring structure, a short flexible chain, and a small but polar headgroup [Bloom et al., 1991]. Figure 1.2C shows the structure of cholesterol (CHOL), the most common sterol in mammalian membranes. Also, the structures of two of its precursors in the synthetic pathway, the desmosterol and ketosterol are showed, together with an artificially demethylated cholesterol (called DCHOL). Other major classes of natural sterols are plant sterols and sterol derivatives, such as the cholesteryl esters.

The lipid content of different membranes and species varies. For example, CHOL content is high in mammalian plasma membranes and in myelin membranes, but it is less abundant in the ER, Golgi, and mitochondria. On the other hand, the highest concentrations of charged lipids are in the mitochondria (25 %) and the plasma membrane (10 %), but glycolipids may

be found almost exclusively in the outer leaflet of the plasma membrane [Sackmann, 1995]. It is worthwhile to note here that most membranes have an asymmetric distribution of lipids in their two leaflets. For example, the outer leaflet of mammalian plasma membranes consist mainly of SM, PC and CHOL, but the inner leaflet has higher concentrations of PE and PS lipids [Zachowski, 1993; Devaux and Morris, 2004]. The asymmetry is usually neglected in studies of model membranes either due to experimental difficulties or in order to simplify the system and the conclusions.

One aspect that partly explains the high variety of lipid species in biomembranes, is that the palette of mechanisms to regulate the fluidity and other physical properties of membranes is very important for the organism. As shall be seen later, sterols are very effective in reducing the fluidity of fluid-like membranes. On the contrary, lipids with polyunsaturated fatty acids (such as the extensively studied ω -3 species) are very effective in increasing the fluidity of membranes [Wassall et al., 2004; Ollila et al., 2007]. The idea behind the regulation is demonstrated by the tendency of the organism to alter the lipid composition of its membranes when environmental parameters, such as temperature, change. For example, the membranes of fish contain higher relative amounts of polyunsaturated lipids during winter than in summer [Ågren et al., 1987], which is an indication of a regulatory mechanism of the fish to keep the fluidity of its membranes constant. Another example is the tight dependence of the regulation of the synthetic pathways of SM and sterols [Futerman and Riezman, 2005].

1.2.2 In Spotlight: Sphingomyelin

When sphingomyelin was first extracted from brain tissue, its biological role seemed as enigmatic as the Sphinx, which resulted to its name [Thudicum, 1884]. Today, we know that in addition to the structural role of sphingolipids in various biological membranes, the products of SM metabolism, such as ceramide, sphingosine-1-phosphate, or diacylglycerol are signal molecules in important cellular processes like apoptosis, ageing and development (for reviews, see for example Huwiler et al. 2000; Cuvillier 2002; Heringdorf et al. 2002). Here, we concentrate on the structural role of SM within lipid bilayers.

The molecular structure of SM resembles closely that of PC, but a few details lead to significant differences in the properties of bilayers that consist of either PC or SM. In particular, the higher saturation state and length of the acyl chain of SM together with the two polar hydrogens in the hydroxyl and

amide moieties of SM are different from PC. Additionally, the double bond of the acyl chain of SM is usually located further away from the headgroup, closer to the bilayer centre.

The properties of one-component SM bilayers differ from those of PC bilayers. For example, the main phase transition temperature, T_m , of most natural SMs is close to the physiological temperature, which is high compared to most natural PCs. However, the phase transition temperature of palmitoyl-SM (PSM, $T_m = 41^\circ\text{C}$) is almost identical to the saturated dipalmitoyl-PC (DPPC) [Koynova and Caffrey, 1995; Bar et al., 1997; Ramstedt et al., 1999]. It has been suggested that other PCs such as 14:0/16:0-PC make a more perfect match with the molecular structure of PSM [Térová et al., 2004], but the T_m remains high for these lipids [Koynova and Caffrey, 1998]. The insertion of a *cis*-double bond has a more significant effect on the T_m of PC than of SM [Koynova and Caffrey, 1995, 1998], which suggests that the intermolecular hydrogen bonding has a role for the phase behaviour of SMs.

The distinct features in the molecular structure of SM may have substantial effects on its interactions with other membrane components such as sterols and proteins. For example, the difference in the nature of the SM-CHOL interaction has been proposed to be more attractive when compared with the interactions of CHOL with other lipids [Silvius, 2003]. This interaction is usually related to the capacity of SM to form intra- and intermolecular hydrogen bonds [Talbot et al., 2000; Veiga et al., 2001] or to the pronounced attractive interaction between the ring-structure of CHOL and chains of SM [Guo et al., 2002; Holopainen et al., 2004]. For the latter, the long and saturated nature of the acyl chains of SM acyl chains may be crucial.

1.2.3 In Spotlight: Cholesterol

Cholesterol is one of the major constituents of eukaryotic membranes. It has been suggested that sterols played a central role in facilitating the evolutionary step from prokaryotes to eukaryotes [Bloom et al., 1991]. In particular, CHOL has been shown to increase the stability of membranes and allow for greater variations in the lipid composition [Vist and Davis, 1990; Bloom et al., 1991]. However, excess free CHOL is toxic, which is why the cell pays a high price in keeping the CHOL levels under tight control. For example, too high concentration of CHOL may cause the loss of membrane fluidity, disruption of membrane domains or cell organelles, or induce apoptosis [Tabas, 2002]. The cell regulates the processes of CHOL biosynthesis, cellular uptake, and efflux, but CHOL is also deposited into fat droplets in

an esterified form. Any disturbance in the network of these intracellular processes leads to a variety of diseases [Simons and Ehehalt, 2002].

The most important function of CHOL is perhaps related to its ability to regulate the physical properties of the membranes [Ohvo-Rekilä et al., 2002]. For a fluid bilayer, the addition of CHOL leads to a more ordered bilayer with increased orientational order of the acyl chains, and increased packing density within the bilayer plane. In addition, CHOL decreases the passive permeability of small solutes through the membrane [Xiang, 1993; Jedlovsky and Mezei, 2003] and suppresses the lateral diffusion of lipids [Hofsäss et al., 2003; Falck et al., 2004]. Perhaps most of these effects are explained by the tendency of CHOL to accommodate itself into the non-polar region of the acyl chains and to reduce the free volume within that region [Falck et al., 2004; Kupiainen et al., 2005].

The ability of CHOL to increase the acyl chain order of physiologically relevant liquid bilayers is based on the smooth and bulky hydrophobic body of the CHOL molecule that packs well with hydrocarbon chains [Silvius, 2003]. However, the situation is more complex because of the different nature of the two opposite faces of the CHOL ring structure. The α -face is smooth, while the two CH_3 groups sticking out from the β -face make it more rough. It has been suggested that saturated acyl chains prefer interactions with the α -face, while unsaturated chains should pack better with the β -face [Pandit et al., 2004a; Róg and Pasenkiewicz-Gierula, 2006a]. Effectively, unsaturated chains have a lower affinity for CHOL than saturated chains, which is further pronounced in the case of polyunsaturation [Pitman et al., 2004].

It makes an interesting subject to compare the effects of CHOL with other sterols. It seems that none of the precursors of CHOL in the synthetic pathway are as effective in ordering acyl chains as CHOL. Comparative studies have been carried out for example for lanosterol, desmosterol, and 7-dehydrocholesterol [Urbina et al., 1995; Smondryev and Berkovitz, 2001; Cournia et al., 2007; Hsueh et al., 2007; Vainio et al., 2006]. Neither has an artificial, completely de-methylated and smoother sterol been able to beat the ordering capacity of CHOL [Róg et al., 2007], let alone any of the the plant sterols studied so far [Schuler et al., 1991; Halling and Slotte, 2004], or possible substitutes for CHOL, such as ceramide [Pandit et al., 2007]. On the basis of the above, it is perhaps surprising that ergosterol, which is common in lower eukaryotes (fungi, yeast), increases the order of saturated acyl chains more effectively than CHOL [Urbina et al., 1995; Smondryev and Berkovitz, 2001; Czub and Baginski, 2006; Cournia et al., 2007; Hsueh et al., 2007]. The difference in sterol composition is possibly explained by the nature of the electrochemical gradients in the different cells. Gradients of ions such

as Na^+ , K^+ , or Cl^- are induced across the plasma membranes of the animal and plant cells, whereas the lower eukaryotes (and cell organelles) have the H^+ gradient. As the leakage mechanisms of these ions across a membrane are different, also different sterols are needed for reducing the leakage [Haines, 2001].

1.3 Phase Behaviour of Lipids

1.3.1 Bilayer Phases

Depending on the shape of the lipids in water solution, they can self-organise into different lyotropic phases, such as micelles, vesicles or bilayers [Israelachvili, 1985]. The bilayer is the favoured structure if the lipids are approximately cylindrical in shape, i.e. the cross sectional area taken by the headgroup is comparable to the area taken by the acyl chains. If the monolayer bending rigidity is low, then even non-cylindrical lipids may be packed into bilayers, but this increases the elastic packing stress and has influences on the lateral pressure profile within the bilayer [Bezrukov, 2000]. In this work, only properties of bilayers are discussed.

The thermotropic behaviour of bilayers is characterised by the main phase transition temperature, T_m , at which the bilayer undergoes a phase transition from the liquid disordered (l_d) phase into the gel or the solid ordered (s_o) phase [Marsh, 1991; Hifeda and Rayfield, 1992] when the temperature is lowered. The l_d phase is typically characterised by low order, fast re-orientational mobility of the acyl chains, fast lateral diffusion of the lipids, and liquid-like arrangement of the headgroups in the plane of the membrane. The gel phase differs from the l_d phase in all of these aspects [Koynova and Caffrey, 1998; Nagle and Tristram-Nagle, 2000]. The area per lipid is lower, which means tighter packing and slower dynamics of the acyl chains. In the gel phase, the acyl chains are almost fully extended and most of the bonds are in the *trans*-conformation. The lipids are hexagonally ordered and the lateral diffusion is strongly reduced when compared to the l_d phase.

In addition to the main phase transition, various sub-transitions may be observed for certain lipids. For example for PCs, the so called rippled gel phase is an intermediate between the low temperature gel phase and the l_d phase [Marsh, 1991]. In addition, the acyl chains in the gel phase may be either tilted or non-tilted, or at lower temperatures, the packing of the chains changes from hexagonal to orthorhombic [Koynova and Caffrey, 1998]. For

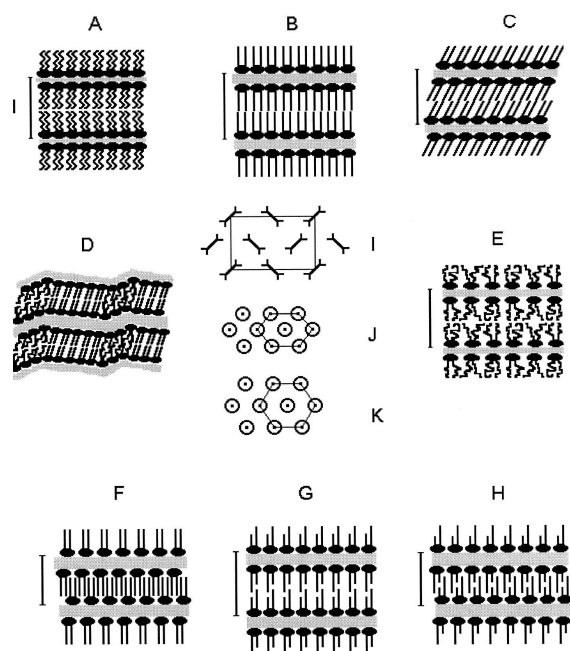


Figure 1.3: Schematics of lipid phases: A) solid ordered, B) gel C) gel with tilted chains, D) rippled gel, and E) liquid disordered phase. The bottom panels display differently interdigitated gel-phases, with: F) full, G) partial, and H) mixed interdigitation. The cross-sectional view of the hydrocarbon chain arrangement in various packing modes: I) orthorhombic, J) quasi-hexagonal, and K) hexagonal. Adapted from [Koynova and Caffrey, 1998].

lipids with significant chain length disparity, typically two types of interdigitated gel phases will be observed. In partial interdigitation, the ends of long chains meet the ends of short chains, whereas in mixed interdigitation, only the ends of the short chains meet. For details see Figure 1.3.

Cholesterol is a unique lipid in that at high concentrations it eliminates the main transition between the gel and the l_d phases, but promotes the liquid ordered (l_o) phase when mixed with other lipids [Ipsen et al., 1987; Bloom et al., 1991]. The mechanism by which this is achieved is that CHOL interacts differently with the translational and the conformational degrees of freedom of lipid molecules [Mouritsen and Jorgensen, 1994]. For the gel phase, CHOL destroys the hexagonal packing, resulting in a more liquid structure. On the other hand, for lipids in the l_d phase, CHOL increases the conformational order of the acyl chains – in this way decreasing the fluidity of the membrane. One should note that high enough CHOL concentration (~ 20 mol-% for DPPC) is needed for the l_o phase, and that with lower concentrations the effects of CHOL are quite different and more local in nature [Mouritsen and Jorgensen, 1994]. At low concentrations, the thermotropic phase of the bilayer is determined by the excess lipid in the mixture. In particular, it has been proposed that CHOL tends to promote the formation of domains of different phases and partition on the interface of these

domains [Mouritsen and Jorgensen, 1994]. One peculiar feature of CHOL at high concentration is that it forms crystals that are laterally segregated from the rest of the membrane [Mason et al., 2003]. For example in ocular lens membranes, increasing amounts of CHOL crystals are formed between molar fractions of 0.6 and 0.8, but not below 0.5 [Epanand, 2003].

1.3.2 Phase Coexistence and Lateral Domains

When more than one lipid species is present in the bilayer, different phase equilibria set in, depending on the mixing properties of the constituent lipids [Mouritsen and Jorgensen, 1994]. In model membranes, various kinds of domains have been measured, depending on the lipid composition and environmental parameters such as temperature [Maxfield, 2002; McConnell and Vrljic, 2003]. In principle, domains or phase separations may be observed in virtually any mixture of more than one lipid component. The lipids of the mixture may differ for example in their chain, headgroup or backbone structure [Faller and Marrink, 2004; Bagatolli, 2006].

Particularly interesting is the perhaps most extensively studied ternary mixture of SM, CHOL, and unsaturated PC such as POPC. The phase diagram of this mixture, as shown in Figure 1.4, includes a variety of coexistent thermotropic phases with relatively low CHOL concentrations [McConnell and Vrljic, 2003]. For example, in Figure 1.4 the physiologically relevant coexistence of the l_o and l_d domains has been shown in the region of relatively high POPC concentrations. Under given circumstances, it has been observed that SM and CHOL separate laterally and form the l_o phase, while the rest of the bilayer is composed of PC in the l_d phase [de Almeida et al., 2005].

In model membranes, depending on the lipid composition and temperature, one may observe either large-scale phase separations or distributions of small transient domains [Almeida et al., 2005]. In Figure 1.4, the dependence of domain sizes on the lipid composition has been indicated, ranging from a few tens of nanometres to over two hundred nanometres [de Almeida et al., 2005]. Recent evidence suggests that the smallest domains consist only of a few molecules and that the domains may condense to form larger domains when parameters such as the temperature are changed [McConnell and Vrljic, 2003].

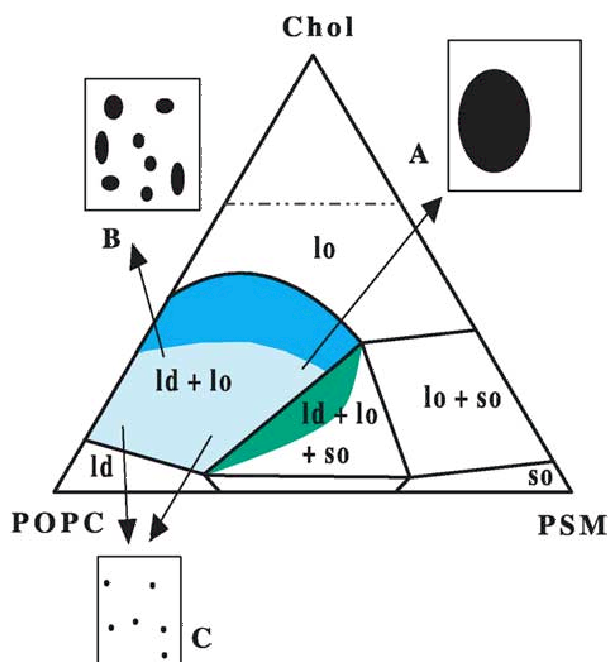


Figure 1.4: Ternary POPC:PSM:CHOL phase diagram, showing the phase boundaries and schematic illustrations of the sizes of lipid domains. The l_d/l_o coexistence area has been indicated with light blue, when the l_d dominates and with dark blue in the opposite case. Adapted from [de Almeida et al., 2005].

1.3.3 Lipid Rafts

Studies on phase separations in model membranes have led to the idea of lipid rafts in biological membranes [Simons and Ikonen, 1997; London, 2005]. The term raft refers to domains of the l_o phase, which are relatively ordered objects floating in a more fluid, l_d environment. Actually, a recently reviewed definition for biomembrane rafts is that they are small (10-200 nm), heterogeneous, highly dynamic, sterol and sphingolipid-enriched domains that compartmentalise cellular processes [Pike, 2006].

Our view of the role of lipids in biological membranes has changed in the past 30 years, since the introduction of the fluid-mosaic model by Singer and Nicolson [Singer and Nicolson, 1972]. The fluid-mosaic model predicted that cellular membranes are fluid, characterised by a random distribution of molecular components in the membrane, resulting in lateral and rotational freedom. The idea of lateral heterogeneities and domains in simple model membranes has been suggested already for over three decades ago [Oldfield and Chapman, 1972; Shimshick and McConnell, 1973], but their possible biological effects, when present in the membranes of living cells, have been understood much more recently, after introduction of the lipid raft hypothesis [Simons and Ikonen, 1997; Edidin, 2003b; Pike, 2004]. Lipid rafts have been suggested to take part in various dynamic cellular processes such as membrane trafficking, signal transduction, and regulation of the activity of

membrane proteins.

The existence of lipid rafts in biological membranes is far from being clear, though, since the lipid rafts, if they do exist, are probably too small to be resolved by most of the currently available experimental techniques [Hancock, 2006; Jacobson et al., 2007]. Despite the progress made in the field lately, the idea of lipid rafts has not yet been fully clarified. For example, we do not know whether actual phase separation or merely a non-random mixing is the best description of biomembranes [Feigenson, 2007]. Direct evidence of rafts *in vivo* is mainly based on monitoring the motions of membrane proteins [Varma and Mayor, 1998; Cottingham, 2004; Simons and Vaz, 2004] or on differential partitioning of fluorescent probes in membrane environments [Gaus et al., 2003]. It is however difficult to perform experiments using living cells, which complicates measurements of physical quantities of the rafts, such as the exact lipid composition, characteristic size, and lifetime [Brown, 1998; London, 2005]. Another related question is the exact nature of the molecular interactions that lead to lipid immiscibilities in membranes, which are also partially unclear [Ramstedt and Slotte, 2002; Holopainen et al., 2004].

Due to the difficulties related to experiments on biomembranes, a number of studies have concentrated on simplified model membranes, such as giant unilamellar vesicles with a few lipid components [Bagatolli, 2006]. Even though these studies provide important information on the physics of lipid membranes, it is not straightforward to relate the results from model membranes to biomembranes. First, model membranes rarely involve other essential components of biomembranes like proteins. One question that arises, is to what extent membrane proteins play a role in inducing and stabilising lipid domains [Epanand, 2004; Hancock, 2006]. Second, some of the model membrane studies are carried out in thermodynamic equilibrium, which is never achieved in a living cell. For example, the energy from ATP is used to maintain the asymmetric lipid composition in the two leaflets of the plasma membrane [Zachowski, 1993], which imposes differential physical properties on the two leaflets. Also, the lipid composition is much more complex in the biomembranes [Edidin, 2003a]. It is not clear, for example, what kind of heterogeneities possibly exist in the intracellular leaflet of the plasma membrane, and to what extent the domains in the two differing leaflets of a membrane may be coupled [Devaux and Morris, 2004; Allender and Schick, 2006]. Also, it is not known what kind of domains might exist in the membranes of cell organelles, such as the ER or mitochondrial membranes [Pike, 2006].

Despite all difficulties, it is worthwhile to continue studies on lipid rafts,

as they might have a very important role for cell biology. For example, a complete understanding of the lipid-protein interactions might be crucially related to many common diseases. Processes such as the immune response [Simons and Ehehalt, 2002], endo- and exocytosis [Schuck and Simons, 2004; Salaün et al., 2004], or intracellular trafficking [Helms and Zurzolo, 2004] have been suggested to be regulated by lipid rafts. Considering the importance of lipid rafts and the high number of related unknowns, together with their estimated small sizes [Varma and Mayor, 1998; Plowman et al., 2005], they make an excellent subject for computational studies.

Research Method

2.1 Classical Molecular Dynamics

2.1.1 The Idea behind MD

The idea behind classical molecular dynamics (MD) dates back at least to the 19th century, when Laplace visioned of a "far-reaching intelligence", which would be able to predict the future by knowing the positions of the constituents of the nature [Schlick, 2002]. The first computer aided implementations of the MD method were developed for statistical mechanics purposes, in order to sample the phase space of systems such as hard spheres [Alder and Wainwright, 1959] or simple fluids [Rahman, 1964]. Since then, MD simulations have been used widely and successfully for different kinds of systems, varying from complex liquids to assemblies of large proteins.

To start an MD simulation, one has to prepare the initial setup by choosing a set of coordinates $\{\vec{x}_i\}$ and momenta $\{\vec{p}_i\}$ for all N particles that comprise the system of interest. The term *classical* refers to the fact that quantum effects are not taken into account explicitly, but the time evolution of the system is entirely determined by Newton's equations of motion:

$$m_i \frac{d^2 \vec{x}_i}{dt^2} = \vec{F}_i = - \frac{\partial U(\{\vec{x}_i\})}{\partial \vec{x}_i}. \quad (2.1)$$

The term U in equation 2.1, the potential energy of the system, is a function of the particle positions $\{\vec{x}_i\}$ and has a key role in determining how the

simulated system evolves in time. If U is carefully chosen, the simulation is an accurate representation of the physical system or process that one wishes to study. To have a long enough simulation *trajectory* at hand, i.e. the positions and momenta of the particles as a function of time, in principle enables the calculation of any classically defined physical property of the simulated system.

In MD-simulation, one is interested in statistical properties of a large number of particles rather than the trajectories themselves. This means that the simulation trajectories need to resemble realistic trajectories in statistical sense. For studies of dynamic properties, the trajectories must be close to the ones of real particles at least over the time scales of the process of interest. Because the simulation trajectory is very sensitive on the initial conditions, any two trajectories that were initially very close to each other will diverge exponentially with time [Schlick, 2002]. In the same manner, two trajectories that have been simulated by slightly different methods, will diverge. Considerable evidence exists that the trajectories produced by MD are representatives of true trajectories in phase-space [Frenkel and Smit, 2002].

Even though the idea behind classical MD is geniously simple, there are complications. First, the choice of the potential U is far from trivial, as discussed in the following sections. Second, equation 2.1 can be solved analytically only for the case $N \leq 2$ [Qiu-Dong, 1991]. Thus, in order to study any practically meaningful physical system, numerical methods are needed to solve the equations of motion. The challenge of solving the equations on computer both as accurately and as effectively as possible has lead to development of a variety of non-trivial algorithms. The aspects of these will be discussed in the following sections.

2.1.2 Force Fields for Biomolecular Systems

In the core of the MD simulation method is the force field, which determines the behaviour of the studied system. In practice, the force field constitutes a set of functions that sum up to the potential energy of the system, U . For example, the potential energy that describes a molecular model, can be written as a sum of different contributions [Schlick, 2002]:

$$U = U_{\text{bond}} + U_{\text{ang}} + U_{\text{tor}} + U_{\text{LJ}} + U_{\text{coul}} \quad (2.2)$$

$$U_{\text{bond}} = \sum_{i,j} \frac{k_{ij}^b}{2} (r_{ij} - r_{ij}^0)^2 \quad (2.3)$$

$$U_{\text{ang}} = \sum_{i,j,k} \frac{k_{ijk}^\theta}{2} (\theta_{ijk} - \theta_{ijk}^0)^2 \quad (2.4)$$

$$U_{\text{tor}} = \sum_{i,j,k,l} \sum_n \left(\frac{V_{nijkl}}{2} [1 + \cos(n\phi_{ijkl} - \phi_{ijkl}^0)] \right) \quad (2.5)$$

$$U_{\text{LJ}} = \sum_{i,j} \left(\frac{B_{ij}}{r_{ij}^{12}} - \frac{A_{ij}}{r_{ij}^6} \right) \quad (2.6)$$

$$U_{\text{coul}} = \sum_{i,j} \left(k \frac{q_i q_j}{r_{ij}} \right) \quad (2.7)$$

In the force-field description above, the energy related to covalently bonded atoms are described by three terms: the bond strain U_{bond} , the angle strain U_{ang} , and the torsional potential U_{tor} . These energy terms are typically described within a single molecule, for atoms that are no further than 1, 2, or 3 covalent bonds away from each other, respectively. The parameter values of the bonded interactions are obtained as a combination of quantum mechanical calculations and experimental methods such as spectroscopic techniques and X-ray crystallography [Schlick, 2002]. Sometimes, special bonded functions are applied. For example, the improper dihedrals are used to fix the planarity or the tetrahedral conformation of certain functional groups. Also, certain force fields use cross-terms in order to improve the performance [MacKerell, 2004].

The two non-covalent terms, U_{LJ} and U_{coul} describe the interactions between all pairs of atoms in the system. The first of these, the Lennard-Jones (LJ) potential, U_{LJ} , is frequently used in force fields of large molecules because of its simplicity [Israelachvili, 1985]. The LJ-potential describes in an average way the attractive London dispersion forces (of the form r^{-6}), together with an effective implementation (r^{-12}) of the hard-core repulsion at short distances. The LJ-parameters may be obtained from fitting simulation results to experimentally available properties such as density of liquid or heat of vaporisation [Berger et al., 1997], or to results from X-ray diffraction [Schlick, 2002]. Often the LJ-interaction is omitted for those atom pairs that are joined by less than three covalent bonds, and sometimes special

LJ-parameters are used for those that are joined by exactly three bonds [van der Spoel et al., 2005].

The last term, U_{coul} is simply the Coulomb interaction between all charged atom pairs. Here, parts of the molecule carry fixed partial charges, generally determined from quantum calculations. It is important to note that the Coulomb potential decays much more slowly with distance than the LJ-potential.

A force field is completely defined by functional forms and parameters, such as the ones represented in equations 2.2 - 2.7. For simulations of biological macromolecules, there is a number of widely used parametrisations available, the main ones originally developed in the 1980s [Ponder and Case, 2003]. The AMBER [Weiner et al., 1984; Cornell et al., 1995], CHARMM [Brooks et al., 1983; MacKerell et al., 1998] and GROMOS-87 [van Gunsteren and Berendsen, 1987] are independent descriptions and were initially developed together with similarly named simulation packages. However, the early origins of virtually all modern force fields may be traced back to the work by Shneior Lifson [Lifson and Warshel, 1968; Levitt and Lifson, 1969]. The development of the OPLS (optimised potentials for liquid simulations) [Jorgensen and Tirado-Rives, 1988] was focused at non-bonded potentials. It was originally used together with other parameters from AMBER, but has later been combined also e.g. with GROMOS-87 [Berger et al., 1997]. All of the above mentioned force fields started with a united atom (UA) description, with nonpolar CH₂/CH₃ groups treated as a single particle. However, recent versions of others but GROMOS have moved to an all-atom (AA) description.

2.1.3 Force Field Parameters in This Work

It is useful to review the history and stages in development of various lipid force fields in order to understand the origins and details of the currently used lipid models, including the lipids used in this work. Here, we concentrate on GROMOS based force-field parameters for lipids.

Early lipid simulations in the 1980s are reviewed for example in [Pastor, 1994]. The first simulations dealt with coarse models of monolayers [Kox et al., 1980], bilayers without water [van der Ploeg and Berendsen, 1982], and small micelles immersed in water [Jönsson et al., 1986]. The first phospholipid simulation that included explicit water molecules was published by Egberts *et al.* [Egberts et al., 1994]. Their model for DPPC was largely

based on the GROMOS-87 force-field. However, their initial choice of parameters resulted in the gel-phase. To reproduce the physically more relevant l_d phase, the authors decided to reduce the partial charges of the lipids by a factor of 2. They also adjusted the vdW-parameters for the CH₂/CH₃ groups and changed the dihedral potential of the acyl chains into the Ryckaert-Belleman (RB) representation in order to more realistically reproduce the structural behaviour of the acyl chains [Ryckaert and Bellmans, 1978]. The adjustments corrected the problem of the wrong physical phase, but left many questions open due to implausible adjustments of the nonbonded interaction parameters.

In 1997, Berger *et al.* published a simulation [Berger *et al.*, 1997], in which they systematically reparametrized the non-bonded interactions used in Egberts' work. Keeping the same bond, angle, and dihedral potentials, Berger *et al.* applied the OPLS parameters for the LJ interactions, earlier used for example in a model for DMPC in combination with AMBER bonded parameters [Essex *et al.*, 1994]. They adjusted the LJ parameters for CH₂/CH₃ groups systematically, by simulating bulk pentadecane and fitting the LJ parameters so that the resulted volume and heat of vaporisation matched with experimental values. In addition to partial charges from OPLS, Berger *et al.* tested another set, calculated by Chiu *et al.* [Chiu *et al.*, 1995], which they found to provide good results. The combination of parameters introduced by Berger *et al.* has been widely used for various phospholipid simulations, the term "Berger lipids" [Tieleman *et al.*, 2006] usually referring to the above discussed combination of GROMOS-87 bonds, angles, and dihedrals (but RB dihedrals for the chains), OPLS for the LJ-interactions (with Berger's adjustments for the chains), and partial charges from the work by Chiu *et al.*

The choice of the water model is closely related to the force field parameters of the lipid model. Though different water models like SPC, SPC/E, TIP4P, and TIP5P [Zielkiewicz, 2005] have been used to model hydrated lipid bilayers, the SPC (simple point charge) model has been recommended to be used in combination with Berger lipids [van Buuren *et al.*, 1993; Tieleman and Berendsen, 1996]. Here, one should note that special reduced LJ-interactions between the water oxygens, O_W, and the CH₂/CH₃ groups have been generally used in combination with the Berger lipids [Berger *et al.*, 1997]. This adjustment was originally based on a study that showed decane to be too soluble in water [van Buuren *et al.*, 1993]. It was later shown that the reduced attraction between water and the acyl chains decreased the area per lipid for a DPPC bilayer, such that it more closely agrees with experimental values [Tieleman and Berendsen, 1996]. Further modifications

have been conducted for the LJ-parameters between water and the polar atoms of DPPC, which affects the hydration of the headgroup [Anézo et al., 2003]. As a consequence, problems may arise when combining the existing parameters for the lipid tails with different headgroups [Róg et al., 2005].

After the lengthy description above, it is finally time to describe the force field of lipids used in this work. The phospholipids (DPPC and POPC) are simply Berger lipids, and had already been used in other studies before [Tieleman and Berendsen, 1998; Patra et al., 2003]. For the *cis*-double bonds, we have used the GROMOS-87 description, though a newer set of parameters [Bachar et al., 2004] has been able to provide more realistic conformations and mobility of the single bonds next to the double bond. However, due to consistency the old description has been used with all simulations of this work. The choice was justified by a test, as shown in *Paper II*, where only minor effects of the double bond parameters on the overall properties of the bilayer were observed.

The model for SM required a few modifications to the force field of PC-lipids due to its distinct features at the interfacial region, see molecular structures in Figure 1.2. The parameters of the amide bond and hydroxyl group in SM were adapted from standard GROMACS building blocks, which in practice means GROMOS-87 parameters [van der Spoel et al., 2005]. Therefore, the bonded interactions of SM are fully compatible with Berger's parametrisation, but for all nonbonded interactions this might not be the case. Actually, the possible discrepancy in LJ-parameters of SM concerns only N and O atoms in the peptide and hydroxyl moieties, respectively. As this involves only two atoms, and the differences in GROMOS-87 and OPLS parameters for these atoms are maximally few tens of percents (for ϵ), it is probably of negligible importance. However, the magnitudes of the partial charges are somewhat lower in the GROMOS-87 building blocks than what are calculated by Chiu *et al.* [Chiu et al., 1995]. By directly applying the GROMOS-87 charges to the two functional groups of SM (all other charges from Chiu *et al.*), we underestimate the strength of the electrostatic interactions in the interfacial region. This might affect our interpretations on the general properties of SM bilayers and on the molecular interactions. Fortunately, other simulation studies with different charges have yielded results very similar to our model [Chiu et al., 2003; Hyvönen and Kovanen, 2003; Mombelli et al., 2003].

The sterol parameters come from the simulation of CHOL by Höltje *et al.* in 2001 [Höltje et al., 2001]. In short, their model for CHOL consists of standard GROMOS-87 parameters, but with increased repulsion between water and carbons. Again, the bonded parameters are fully compatible

with the Berger lipids, but the non-bonded are not. The LJ-parameters in GROMOS-87 are more attractive than in OPLS. Also, the weak partial charges at the OH-group are compatible with our SM-model, but not necessarily with Berger's PC-lipids with partial charges from Chiu *et al.* [Chiu *et al.*, 1995]. Again, these discrepancies in non-bonded parameters may result in non-balanced molecular interactions when PC, SM and sterols are mixed. However, the combination of Berger's PC lipids and Höltje's CHOL have been used in numerous studies [Falck *et al.*, 2004; Pandit *et al.*, 2004a; Patra, 2005] and they have yielded results in agreement with experiments and the simulations conducted in this work.

2.1.4 Integrating Equations of Motion

The choice of *integrator*, i.e. the numerical algorithm to solve the equations of motion at discrete time intervals, has an important effect on the efficiency and accuracy of the simulation. In this work, a version of the widely used Verlet scheme, the so-called leapfrog integrator [Schlick, 2002] has been used, as implemented in the GROMACS package [van der Spoel *et al.*, 2005]:

$$\vec{v}(t + \frac{\Delta t}{2}) = \vec{v}(t - \frac{\Delta t}{2}) + \frac{\vec{F}(t)}{m} \Delta t, \quad (2.8)$$

$$\vec{r}(t + \Delta t) = \vec{r}(t) + \vec{v}(t + \frac{\Delta t}{2}) \Delta t. \quad (2.9)$$

Importantly, the leapfrog algorithm is simple and computationally very efficient, but it also preserves two essential properties of Hamiltonian systems. Time-reversibility and preservation of the volume in phase space are generally considered to be good properties of integrators [Frenkel and Smit, 2002; Schlick, 2002]. Although the leapfrog scheme provides only a fair short-term energy conservation, the long-term energy drift is small, which is actually more important for molecular simulations. More accurate integrators are used for example in modelling the dynamics of planetary systems [Hockney and Eastwood, 1988; Ito and Tanikawa, 2002], which aim to high-accuracy trajectories. Molecular simulations aim to produce average properties of ensembles of atoms/molecules instead of exact trajectories, and thus the high numerical accuracy of the integrators will be less important.

2.1.5 Constraints

The harmonic potentials in interactions of equations 2.3 and 2.4 lead to oscillations. The highest frequency wavenumbers are typically in the order of 3700 cm^{-1} for the stretching of the O-H bond, and 1000 cm^{-1} for the C-C bond, while the highest angle bending modes are around 1600 cm^{-1} , 1500 cm^{-1} , and 300 cm^{-1} for H-O-H, H-C-H and C-C-C angles, respectively [Schlick, 2002]. The classical limit for energy, $k_B T > h\nu$, suggests that the classical treatment for bonds and angles may be problematic for wavenumbers higher than 100 cm^{-1} and corrections should be implemented to the energy terms [van der Spoel et al., 2005].

Another possibility is to remove the vibrational degrees of freedom by constraining the bond lengths and angles with an algorithm such as SHAKE [Ryckaert et al., 1977]. In practice, an algorithm called SETTLE [Miyamoto and Kollman, 1992] is used specifically for water to constrain the bond length and angle vibrations. For large molecules like lipids, the linear constraints solver (LINCS) is used [Hess et al., 1997]. After constraints, the highest frequency mode in the system is the H-C-H angle vibration, 1500 cm^{-1} . Considering that a reasonable integration time step must be about one tenth of the period of the highest mode, this limits the available timestep down to about¹ $\Delta t = 2\text{ fs}$. Without constraints, one would need a much smaller timestep of about $\Delta t = 0.9\text{ fs}$. In this work, we have always used SETTLE for water, LINCS for the lipids and a time step of 2 fs.

2.1.6 Boundary Conditions and Ensemble

The available computer power sets the upper limit for the size of the simulated system. For example, a relatively large MD-simulation today might cover about 100.000 atoms. If the atoms were packed in a cubic box, about 13 % of them² would lie at the boundaries of the box, which implies problems when compared to an experimental system of any realistic practical size. To reduce these effects, periodic boundary conditions (PBC) are frequently used [Allen and Tildesley, 1990] in simulations to mimic an infinite bulk system. For lipid bilayers, the usage of PBC means simulating an infinite stack of alternating layers of lipid and water.

Another boundary condition needed to map the simulation to an experiment is the chosen thermodynamic ensemble. In the simplest case, one may just

¹A measured wavenumber $k = 1500\text{ cm}^{-1}$ means a vibration frequency of about $4.5 \times 10^{11}\text{ Hz}$ or a period of $22 \times 10^{-15}\text{ s} = 22\text{ fs}$.

²The number of atoms at the surface: $6 \times 100.000^{2/3}$

employ the PBC and solve the equations of motion. This would lead to the NVE-ensemble, which corresponds to a thermally isolated system with constant particle number (N), volume (V), and total energy (E). However, much more convenient from experimental point of view is the NPT-ensemble, which maintains a constant pressure and temperature.

The temperature is kept constant with a specific algorithm called *thermostat*. A simple and efficient way is to use the so-called weak coupling scheme by Berendsen [Berendsen et al., 1984]. A desired temperature T_0 is obtained by slightly scaling the velocities of each particle at each time step so that the temperature will be corrected according to:

$$\frac{dT}{dt} = \frac{T_0 - T}{\tau}. \quad (2.10)$$

Even though the weak coupling scheme is very effective in bringing the average temperature of the system to T_0 , it has not been explicitly proven to produce any thermodynamic ensemble correctly [van der Spoel et al., 2005]. In order to properly simulate an ensemble with constant temperature, one should apply a theoretically more correct thermostat, like the one by Nosé and Hoover [Nosé, 1984; Hoover, 1985]. This scheme is based on reformulating the Hamiltonian of the system such that the velocities of the particles are coupled to an external heat reservoir through a frictional term ξ :

$$\frac{d^2 \vec{x}_i}{dt^2} = \frac{\vec{F}_i}{m_i} - \xi \frac{d\vec{x}_i}{dt}, \quad (2.11)$$

where a parameter Q is chosen such that the friction is adjusted according to $d\xi/dt = (T - T_0)/Q$. The Nosé-Hoover thermostat has been shown to produce the correct NVT-ensemble although care should be taken when adjusting the parameters in order to avoid artefactual long-term oscillations of the kinetic temperature [Holian et al., 1995].

To achieve the NPT ensemble, we first need to define the pressure tensor \mathbf{P} of the system,

$$\mathbf{P} = \frac{1}{V} \left(\sum_i^N m_i \vec{v}_i \otimes \vec{v}_i + \sum_{i<j} \vec{r}_{ij} \otimes \vec{F}_{ij} \right), \quad (2.12)$$

where V is the box volume, the first sum corresponds to the total kinetic energy of the system and the second to the virial [van der Spoel et al., 2005].

A *barostat* is needed to keep the pressure constant. For example, a similar approach to the weak temperature coupling scheme is the Berendsen barostat [Berendsen et al., 1984], which simply scales the dimensions of the simulation box in order to achieve the reference pressure \mathbf{P}_0 . A more sophisticated barostat is the Parrinello-Rahman scheme [Parrinello and Rahman, 1981; Nosé and Klein, 1983], which is based on the extended ensemble and is analogous to the Nosé-Hoover thermostat. For a rectangular box, it is the diagonal elements of the pressure tensor \mathbf{P} that account for the scaling. Typically, one treats the system either isotropically (all dimensions scaled by the same amount) or anisotropically (all directions scaled independently).

For bilayer simulations, another important ensemble is the $N\gamma T$, in which the surface tension, γ , is kept constant instead of the bulk pressure. By definition, the surface tension can be calculated from the difference of the normal and lateral pressures: $\gamma(t) = L_z[P_{zz} - (P_{xx} + P_{yy})/2]$. The $N\gamma T$ ensemble may be realized by applying the barostat semi-isotropically, so that the normal direction (z) and the lateral dimensions (x, y) are coupled separately.

The wide usage of the Berendsen thermostat and barostat is generally defended by the fact that the coupling affects the particle dynamics only very weakly [van der Spoel et al., 2005] and that the results are very similar when compared to the extended ensemble schemes [Anézo et al., 2003]. However, it is at least theoretically problematic to analyse dynamic quantities or fluctuations from a simulation, if one does not know which ensemble it represents.

All results presented in this work have been obtained by employing the $N\gamma T$ ensemble with $\gamma = 0$. The Berendsen/Berendsen scheme has been always used for equilibration purposes, after which the Nosé-Hoover/Parrinello-Rahman have been usually switched on to get the correct ensemble. It is worthwhile to stress that if one is interested in volume or area fluctuations in the simulated systems, it is important to use the theoretically correct coupling scheme.

2.1.7 Treatment of Electrostatics

In practice, almost all important biological molecules are either polar or charged [Nelson and Cox, 2005]. For example, the headgroup of a PC-lipid (Figure 1.2) contains two full electronic charges situated relatively close to each other. The molecular charges cause both strong specific interactions like hydrogen bonding, and coupled effects like the regulation of the bilayer area through dipole-dipole interactions of the headgroups [Wohlert and Edholm,

2004]. Therefore it is worthwhile to consider with great care how to handle the electrostatic interactions in the simulations properly.

The size of the simulation box sets the upper limit for the range of any pairwise interaction. In the simplest case, one could use a chosen cutoff distance r_c and calculate the interaction energy of charged atom pairs within that distance, forgetting all other pairs. Because of its simplicity, the cutoff method has been widely used. Recently, however, it was shown for DPPC bilayers that the simple cutoff scheme induced significant structural artefacts exactly at the cut-off distance. The problem persisted even for relatively long cutoff-distances ($r_c = 2.5$ nm), and also differences in important structural properties like area per lipid were observed as a function of the r_c value [Patra et al., 2003]. Later, detailed studies have revealed that the quality of the results with the simple cutoff scheme depends strongly on the details of the implementation, particularly on the choice of the *charge groups* [Róg et al., 2003; Wohlert and Edholm, 2004]. Due to the sensitivity of the cutoff-method for the details of the implementation [Wohlert and Edholm, 2004], great care should be used or alternative methods should be considered.

The Onsager reaction field technique [Onsager, 1936] has been shown to be a good method in lipid simulations, since it is very effective and overcomes the coarse problems of the simple cutoff scheme. The reaction field technique involves a cutoff-distance as well, but beyond r_c the electrostatic interactions are treated in a mean-field manner, described by the dielectric constant ϵ_{rf} . The modified interaction reads:

$$V(r) = \frac{q_i q_j}{4\pi\epsilon_0 r} \left[1 + \frac{\epsilon_{\text{rf}} - 1}{2\epsilon_{\text{rf}} + 1} \left(\frac{r}{r_c} \right)^3 \right] - \frac{q_i q_j}{4\pi\epsilon_0 r_c} \frac{3\epsilon_{\text{rf}}}{2\epsilon_{\text{rf}} + 1}, \quad (2.13)$$

where the first term does the job and the second term brings the potential to zero at $r = r_c$. In particular for some uncharged systems, the results of the reaction field method have been shown to be as reliable as those of PME (see below), but the reaction field scales much more effectively in parallel computing environments [Patra et al., 2007]. The problem of choosing the right value for the parameter ϵ_{rf} in a lipid/water interface is theoretically tricky, but practically of less importance: the values of $\epsilon_{\text{rf}} = 80$ (water) and $\epsilon_{\text{rf}} = 4$ (nonpolar region) lead to the values of 0.49 and 0.33, respectively, for the prefactor of $(r/r_c)^3$ in equation 2.13.

Another choice is to consider the total electrostatic energy of the system without the usage of any kind of cutoffs. Formally, the infinite summation over all charges and periodic boxes is conditionally convergent for a neutral

system and it can be calculated either with the classical Ewald summation method [Ewald, 1921] or with the Particle Mesh Ewald (PME) method [Darden et al., 1993; Essmann et al., 1995]. The efficiency of the algorithms scales with particle number N as $\mathcal{O}(N^{3/2})$ for Ewald and $\mathcal{O}(N \log N)$ for the PME. The Ewald method is suggested to enhance the artificial periodicity of very small systems, but the effect is actually a consequence of the PBC. Additionally, the effect is probably negligible for systems that are solvated in water and larger than a few nanometres in size [Smith and Petitt, 1996; Weber et al., 2000]. For simulations today, PME is considered to provide the most reliable results [Patra et al., 2003; Róg et al., 2003; Cordero et al., 2007], the major downside being the relatively poor scaling on certain parallel computing environments [Patra et al., 2007].

In this work, PME has been used in most of the simulations. The only exception are the large-scale simulations in *Paper V*, which were simulated with the reaction field technique in order to increase the computational efficiency.

2.1.8 Limitations and Considerations

The main limitations of the standard MD-simulation method are the limited computational power, the complexity of the force field, and the poor treatment of quantum effects such as polarisability [Tieleman et al., 1997]. Additionally, numerous questions arise from the implementation and correct choice of the algorithms. Since MD-simulations are routinely used in studies of molecular systems, care should be taken to acknowledge the possible limitations of the method before reporting results. Here, the most worrying aspects related to lipid simulations are reviewed.

The maximum available timestep sets a practical limit for the length- and timescales of a simulation. Processes whose characteristic times are exceeded by the simulation length may be studied with adequate statistics. Such processes are typically chain rotations (10 ps to 1 ns), headgroup rotations (few ns), lipid protrusions (ns), or lipid rotations (tens of ns). Also lateral diffusion and conformational organisation of lipids may be studied, but typically at a maximum length scales of nanometres. For example, the undulation modes smaller than system size are covered [Lindahl and Edholm, 2000a]. However, many highly relevant and interesting aspects, like the complete mixing in a multicomponent bilayer or the flip-flop across the bilayer centre are completely beyond the range.

If we assume that the popular Moore's Law [Moore, 1965] holds for a few

more years, one can extrapolate to the future. The same computer power as in year 2000 allowed a 10 ns simulation of 1024 lipids [Lindahl and Edholm, 2000a], would in year 2021 allow about 160 μs simulation of the same bilayer or about 1.6 μs of 100.000 lipids. This is of course much better than what can be done today, but one is still restricted at the left end of the biological length-scale, as introduced in Figure 2.1. For example, simulating a whole cell organelle in full atomic detail will be a distant dream for decades. Therefore, to widen the spectrum of applicable problems, one should not only wait for the increase in computer power but try to tackle available problems by asking clever questions and to continue the development of more efficient algorithms and faster simulation methods. This is fortunately being done continuously, various coarse grained (CG) models have for example recently been introduced for biomolecular systems [Ayton and Voth, 2002; Marrink et al., 2004; Murtola et al., 2004; Gao et al., 2007]. Also, algorithms such as multiple time-step integrators are being developed [Feenstra et al., 1999].

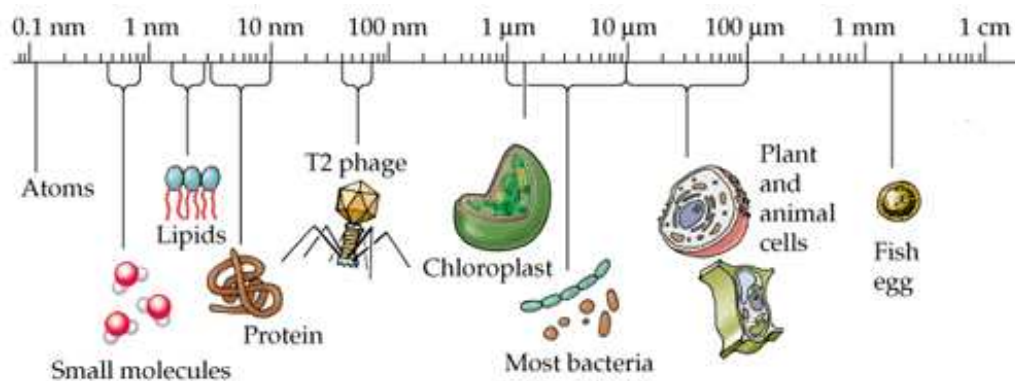


Figure 2.1: Various length scales of biological systems. Adapted from [Purves et al., 2004].

Closely related is the question of how to determine the system size in simulation. For some situations a small system is ideal, as one can reach longer timescales and consequently better statistics. But on the other hand, reducing the size of the simulation box might also lead to serious finite size artefacts. In particular, small systems have been reported to produce too packed and ordered bilayers [Lindahl and Edholm, 2000a; de Vries et al., 2005] and slower lateral diffusion [Klauda et al., 2006]. The effects due to artificial enhancement of periodicity in small systems will be suppressed and the calculated properties have been shown to converge for systems larger than 36 lipids per leaflet [de Vries et al., 2005]. For significantly larger systems, new phenomena such as undulations start to emerge and affect mea-

sured properties, which is a completely separate issue [Lindahl and Edholm, 2000a].

The system size is greatly affected by adequate hydration. If the simulation is to be compared with experiment in excess water, enough water molecules should be taken into the simulation as well. Having too little water between the periodic images of the bilayer also reduces the area per lipid and slows down diffusion [Mashl et al., 2001; Anézo et al., 2003; Högberg and Lyubartsev, 2006], but it also has dramatic effects on the conformations and the dynamic behaviour of the lipid headgroups [Högberg and Lyubartsev, 2006]. Though the PC-headgroup accommodates about 12 water molecules in its hydration shell [Mashl et al., 2001], the limit of full hydration of a bilayer is usually considered to be much higher, about 20-30. A factor that should further increase the minimum amount of water, is the inclusion of ions into the solution. As biological solutions are always ionic and as the presence of salt has been shown to alter the properties of neutral PC-lipids [Böckmann et al., 2003], it is relevant to ask whether ions should be included in all simulations. Where most of the MD-simulations of proteins are surrounded by a physiological salt solution [Ibragimova and Wade, 1998], almost all lipid studies are carried out in pure water.

Simulations of single component bilayers in the l_d phase are the simplest and allow for most reliable statistics, which is why most lipid simulations have concentrated on single component bilayers. Although studies reporting properties of the gel-phase [Tu et al., 1996; Sun, 2002; Čurdová et al., 2007], and the l_o phase [Hofsäss et al., 2003; Falck et al., 2004] exist, the slow dynamics usually renders the interpretation difficult. Also, studies of temperature effects have been extremely rare, but recently increasing computing power has allowed studies that aim to reproduce the phase transitions between gel and fluid phases [Marrink et al., 2005; Leekumjorn and Sum, 2007]. In addition, the phase behaviour of lipids in non-bilayer phases have been studied [Marrink and Mark, 2004; Knecht et al., 2006]. Here, care should be taken when choosing the proper algorithmic set. For example, different methods of barostat coupling (anisotropic/isotropic) have been shown to drive the system towards different phases (bilayer/micelle) [Patel and Balaji, 2005]. Another highly interesting direction of new simulation studies is towards more realistic systems, such as asymmetric bilayers [Cascales et al., 2006; Gurtovenko and Vattulainen, 2007]. Though theoretical and applicational problems are still related to simulating these systems, it is highly encouraging to see how quickly the history of simulations has been proceeding.

The second major limitation is related to the force fields. The large number of parameters to describe a force-field and the number of various parameter

sets available makes the choice very complex. Different parametrisations have been developed gradually during tens of years and always in combination with certain algorithms or boundary conditions. Although the parameters and functional forms are usually openly available, some historical aspects or critical factors are not obvious or are not explicitly stated. For example, the widely used Berger-parameters for lipids [Berger et al., 1997] are partly based on the GROMOS-87 force field, whose origins and derivation "have never been documented completely" according to the developers [van Gunsteren et al., 1998]. Another topical issue is related to the lipid-protein interactions. As the force field parameters for proteins and lipids have been mostly developed separately in the past, a proper combination of these two in the same simulation is far from trivial [Tieleman et al., 2006].

The quality of the force field is usually justified by comparing properties such as area per lipid between simulation and experiment. However, as pointed out by Anézo *et al.* [Anézo et al., 2003], the right combination of force field and methodology can always reproduce the desired area, which alone is therefore not necessarily a good measure for the quality of the force field or the method. Also, as most of the measurable properties in a simple, one-component bilayer are a function of the area per lipid, it is easy to understand that simulations with various force fields and methods lead to similar results. It is useful to keep in mind that even if the results themselves are probably in order, they may be so for the wrong reasons, because the balance of forces within the bilayer may be wrong. However, as the methods to calculate and (indirectly) measure the pressure profiles across the bilayer are developing [Lindahl and Edholm, 2000b; Sonne et al., 2005; Ollila, 2006], future will bring more detailed tools for validation of the simulation results against experimental data.

The very nature of classical MD is to forget quantum effects, or at best, implement them in an average way. The latter is the case for example for static partial charges used in biomolecular force fields. Also, chemical reactions or effects of pH cannot be modelled explicitly, but separate molecular topologies need to be created for each environmental condition. Even though structural properties of e.g. hydrogen bonding liquids have been adequately reproduced by classical models, better implementation of quantum effects such as atomic polarisability may be crucial for accounting for many other effects. It is interesting to see that development toward these ideas is on the way, for example algorithms for polarisable force fields or for combined quantum/classical simulations have already been included in the GROMACS package, though their extensive testing or available parametrisations are still lacking.

2.2 Simulation vs. Experiment

2.2.1 Structure from Diffraction

X-ray and neutron diffraction experiments are widely used to measure the structure of lipid bilayers [Nagle and Tristram-Nagle, 2000]. Typically, experiments are carried out for stacks of hydrated bilayers with a repeat distance D , and the low-angle diffraction is measured. From the result, the form factor $F(q)$ of one bilayer may be constructed. For symmetric bilayers, the form factor is further defined by [Klauda et al., 2006]:

$$F(q) = \int_{-D/2}^{D/2} [\rho(z) - \rho_w] \cos(qz) dz, \quad (2.14)$$

where $\rho(z)$ is either the electron density profile (X-rays) or the mass density profile (neutrons) across the bilayer and ρ_w is the corresponding density of water. The z -axis here is normal to the bilayer.

The distance of the main peaks in the density profile (due to headgroups) may be used to estimate the thickness of the bilayer, and, assuming a value for the volume per lipid, to estimate the average area per lipid [Nagle and Tristram-Nagle, 2000; Tristram-Nagle and Nagle, 2004]. From simulation, the density profiles can be calculated directly and compared with the experimental ones. Also, values for the area per lipid are computed from the dimensions of the simulation box and compared with the values from diffraction studies. Usually the aim here is to validate the parameters of the model, but as the measurement of the area per lipid involves assumptions, and the measured values for the area per lipid vary [Nagle and Tristram-Nagle, 2000], it would perhaps be more accurate to compare the bilayer structure factors directly in the reciprocal space [Benz et al., 2005; Kučerka et al., 2006].

In principle, the in-plane structure of lipid membranes may also be gauged by diffraction, such as inelastic neutron scattering experiment [Rheinstädter et al., 2006]. However, the resolution of the technique does not allow for studying e.g. lateral domains in a single membrane, but stacks need to be used here as well. Little more than the nearest-neighbour distance of the lipid acyl chains has been measured so far.

2.2.2 Order and Dynamics from NMR

Nuclear Magnetic Resonance (NMR) technique has been widely used to determine the average structure and dynamics of lipid molecules within a

bilayer. For example, the order parameter of a carbon-deuterium (C-D) bond in a deuterated acyl chain, S_{CD} , is obtained from the quadrupolar splitting, $\Delta\nu$, of the NMR spectrum:

$$S_{\text{CD}} = \frac{1}{2} \langle 3 \cos^2 \theta - 1 \rangle = \frac{4}{3} \left(\frac{h}{e^2 q Q} \right) \Delta\nu, \quad (2.15)$$

where ($e^2 q Q / h = 170 \text{ kHz}$) is the static quadrupole coupling constant for C-D bonds and θ is the angle between the magnetic field and the C-D bond [Seelig and Seelig, 1974]. The deuterium order parameters are highly useful in that they can be directly compared with simulation [Petrache et al., 2000]. From simulation with united atoms, one usually calculates the order parameters either on the basis of the chain backbone conformations [van der Spoel et al., 2005], or by first adding hydrogens to their geometrical equilibrium positions and calculating the order parameter from the definition in equation 2.15.

The dynamics of the acyl chains may be obtained from the NMR spin-lattice relaxation times T_1 . For example, for the C-D bonds of lipids in vesicles [Lindahl and Edholm, 2001; Mashl et al., 2001], the spin-lattice relaxation rate is given by:

$$\frac{1}{T_1} = \frac{3\pi}{10} \left(\frac{e^2 q Q}{\hbar} \right)^2 [J(\omega_D) + 4J(2\omega_D)], \quad (2.16)$$

where ω_D denotes the nuclear Larmor frequency of ^2H , and $J(\omega)$ is the spectral density of the second rank reorientational autocorrelation function, $C_2(t)$. The situation is defined by two equations:

$$J(\omega) = \int_0^\infty C_2(t) \cos(\omega t) dt, \quad (2.17)$$

$$C_2(t) = \frac{1}{2} \langle 3[\vec{\mu}(t) \cdot \vec{\mu}(0)]^2 - 1 \rangle, \quad (2.18)$$

where $\vec{\mu}$ is the unit vector along the C-D bond. The above relation is important, as the $C_2(t)$ function may be directly extracted from simulation for any selected bond. The above discussion is not only limited to acyl chains, but order parameters and relaxation times of deuterated head group regions may be measured. NMR results for other nuclei may also be calculated from simulation in a similar manner, such as ^{13}C for the C-H vectors [Lindahl

and Edholm, 2001; Feller et al., 2002; Pastor et al., 2002], or the ^{14}N for the headgroup vector [Siminovitch and Jeffrey, 1981].

Molecular motions of different time scales contribute to the decay time of the correlation function $C_2(t)$. The fastest motions are related to the *gauche/trans* isomerisation of the acyl chains, which are of the order of 50-100 ps, whereas the molecular rotations and wobble are in the range of nanoseconds [Pastor and Feller, 1996]. Various methods, such as multi-exponential fits are used to characterise the shape of the correlation function from simulation [Pastor and Feller, 1996; Mashl et al., 2001; Pitman et al., 2005], or as in equation 2.17, a Fourier transform has been conducted for the correlation function to yield the experimentally measurable T_1 relaxation time [Feller et al., 2002; Wohlert and Edholm, 2006] In this work, we have merely characterised the decay of the $C_2(t)$ functions by defining the effective correlation time:

$$\tau_{\text{eff}} = \int_0^{\infty} dt \frac{C_2(t) - C_2(\infty)}{C_2(0) - C_2(\infty)}, \quad (2.19)$$

which gives a reasonable estimate for the overall decay in question [Pastor et al., 2002]. One may note here that the plateau value of the correlation function is related to the order parameter by $C_2(\infty) = |S_{\text{CD}}|^2$ [Pitman et al., 2005].

2.2.3 Lateral Diffusion

An important dynamic quantity of a bilayer is the lateral diffusion coefficient, D_T , of the lipid molecules. Experimentally, this quantity can be determined for example from single-molecule tracking [Fujiwara et al., 2002], pulsed-field gradient NMR [Orädd and Lindblom, 2004], fluorescence correlation spectroscopy [Schwille et al., 1999], and fluorescence recovery after photobleaching (FRAP) [Almeida et al., 1992], which all operate on the millisecond time scale and give typically similar results [Wohlert and Edholm, 2006]. On the other hand, neutron scattering experiments operate in the picosecond range and give significantly higher diffusion rates [König et al., 1992].

There are a number of issues related to calculating diffusion coefficients from simulation. The first limiting factor is the available time-scale and poor sampling due to low number of molecules, which often makes comparison to experiments difficult [Wohlert and Edholm, 2006]. One should note that the diffusive behaviour of the lipids may be obtained only after long enough

times [Frenkel and Smit, 2002; Wohlerlert and Edholm, 2006]. Typically, the diffusion coefficient is determined from the mean-squared displacement of the lipid positions,

$$D_T = \lim_{t \rightarrow \infty} \frac{1}{2dt} \langle [\vec{r}(t)]^2 \rangle, \quad (2.20)$$

where $d = 2$ is the dimensionality of the diffusion. Here, the random relative motion of the two lipid monolayers can lead to apparent super-diffusive motion of the individual molecules if not taken into account [Anézo et al., 2003]. This is clearly an artefact due to small system size, as the effect vanishes for large systems [Klauda et al., 2006]. For small systems, the correct diffusion coefficient may be calculated by removing the monolayer movements first.

2.2.4 Elasticity

The large-scale behaviour of an undulating membrane may be described by the Helfrich bending free energy [Safran, 1994]:

$$F_{\text{bend}} = \int dA \left[\frac{1}{2} k_c (H - H_0)^2 + k_g H_G \right], \quad (2.21)$$

where $H = 1/R_1 + 1/R_2$ is the sum of the two local principal curvatures, H_0 is the spontaneous curvature of the membrane, k_c is the bending rigidity modulus, $H_G = 1/R_1 R_2$ is the Gaussian curvature, and k_g is the corresponding modulus. The integral covers the membrane area. For symmetric bilayers, H_0 vanishes and the Gaussian curvature term contributes a constant and can thus be neglected from the integral [Safran, 1994]. More details on how to analyse undulations from simulation is included in the last chapter of this thesis.

Another typical way to characterise membrane elasticity is to look at the compression in the plane of the membrane. The derivative of free energy F with respect to membrane area A defines the surface tension of the lipid-water interface [Feller and Pastor, 1996],

$$\gamma = \left(\frac{\partial F}{\partial A} \right)_T. \quad (2.22)$$

In vicinity of the equilibrium area A^* , changes in free energy may be expressed through series expansion: $\Delta F = \frac{1}{2}F''(A^*)(A - A^*)^2$, which leads to a connection between the area fluctuations and the area compressibility modulus:

$$K_A \equiv A \left(\frac{\partial \gamma}{\partial A} \right)_T = k_B T \frac{A}{\langle \delta A^2 \rangle}, \quad (2.23)$$

where the denominator $\langle \delta A^2 \rangle$ is the variance of the fluctuating membrane area, as available directly from the simulation.

2.2.5 Lateral Pressure Profiles

To understand the balance of forces within a bilayer and the nature of surface tension, it is useful to modify the expression for the pressure tensor in equation 2.12 such that it is defined locally. In particular, one can divide the simulation box into horizontal slices in z -direction and calculate the average pressure tensor within each slice [Lindahl and Edholm, 2000b]:

$$\mathbf{p}(z) = \frac{1}{A_p \Delta z} \left[\sum_{i \in \text{slice}} m_i \vec{v}_i \otimes \vec{v}_i + \sum_{i < j} \vec{r}_{ij} \otimes \vec{F}_{ij} g(z, z_i, z_j) \right], \quad (2.24)$$

where $A_p \Delta z$ is the volume of the slice. The first sum includes all atoms within the slice, but the second sum has also contributions from atoms that are outside of the slice. The function g determines to which extent atom pair (i, j) contributes to the virial of the slice. The Irving-Kirkwood contour method [Irving and Kirkwood, 1950] draws the shortest line between atoms i and j , and divides the virial contribution linearly to all slices along the line. For more details, possible problems and limitations of the implementation may be found from [Lindahl and Edholm, 2000b; Sonne et al., 2005].

After defining the local pressure tensor as in equation 2.24, we may define the lateral pressure profile as the difference of the average lateral p_L and normal p_N pressure components in the slice at z :

$$\Omega(z) = p_L(z) - p_N(z) = \frac{p_{xx}(z) + p_{yy}(z)}{2} - p_{zz}(z). \quad (2.25)$$

The negative sign of Ω means that the bilayer tends to shrink in the xy -plane and the positive sign means a tendency to expand. By integrating

the lateral pressure profile across the whole system, one gets a value for the macroscopic, measurable surface tension:

$$\gamma = - \int dz \Omega(z). \quad (2.26)$$

The importance of the lateral pressure profile is further pronounced by the fact that it is coupled to a number of other macroscopic properties. For example the quantities presented in equation 2.21, such as the spontaneous curvature, H_0 , the bending rigidity modulus, k_c , and the saddle-splay modulus, k_g , may be directly derived from the $\Omega(z)$ [Ben-Shaul, 1995; Safran, 1994]. In addition, the changes in the distribution of pressure within a membrane have been suggested to be significant for regulating the activity of membrane proteins [Cantor, 1999].

In theory, the lateral pressure profile would provide an excellent way for coupling the microscopic information from simulation with macroscopic information from experiments. However, even though the shape of lateral pressure profile has recently been determined in a number of studies and the importance of the concept has become more accepted, there are still a number of open questions [Sonne et al., 2005; Ollila, 2006]. For example, the precise form of the lateral pressure profile and its dependence on lipid composition are yet unclear. Only one attempt exists to experimentally gauge the lateral pressure within a membrane [Templer et al., 1998]. In their work, the authors used a fluorescent probe to compare the relative lateral pressures at four different locations of the hydrophobic part of a membrane. So far, no one has measured the quantitative values of the pressure profile.

2.3 Systems Studied in This Work

In *Paper I* and *Paper II*, all studied bilayers consist of 128 SM molecules and 3655 water molecules. The simulations were carried out in a temperature of 323 K, using the Nose-Hoover thermostat and in a tension free state using the semi-isotropic Parrinello-Rahman barostat. All simulations were 50 ns in duration.

In *Paper III*, we study seven different mixtures of DPPC or POPC with different sterols (20 mol-%) and compare them with properties of one-component DPPC or POPC bilayer simulations. The other simulation parameters are identical to the above, but the duration of the simulations is 100 ns, and for the baro- and thermostat, we use the Berendsen scheme.

All three systems studied in *Paper IV* and *Paper V* consist of 1024 lipids with the molar fractions of POPC:PSM:CHOL = 1:1:1, 2:1:1, and 62:1:1. All of the systems were discussed in *Paper V*, but only the third one in *Paper IV*. The simulation time was 50 ns for the third system and 100 ns for the other two. The temperature (310 K) was kept constant with the Nose-Hoover scheme, and the pressure with the semi-isotropic Parrinello-Rahman. For the pressure profiles presented in *Paper V*, a few selected simulations (128 lipids each) from previous works were included for comparison: PSM, POPC, and DPPC:CHOL.

CHAPTER 3

Properties of Sphingomyelin

3.1 Motivation

This chapter discusses the characteristic features of SM: the high hydrogen bonding capacity, the high degree of saturation of the acyl chains, and the high variety in the length of the acyl chains. The discussion is based on *Paper I* and *Paper II*.

First, the most important bilayer properties of 16:0-SM (PSM) will be compared with a structurally very similar PC (di-16:0-PC, DPPC), perhaps the most studied lipid of all. In addition to bringing important insight about the properties of these bilayers and about the hydrogen bonding characteristics of SM, the comparison serves as a validation for the SM model used in this work. In the end of the chapter, different molecular species of SM are compared with each other and the effects of chain length and unsaturation on bilayer properties are discussed.

3.2 Comparison of PSM with DPPC

Perhaps the most evident difference in one-component bilayers consisting of either PSM or DPPC are the bilayer dimensions. Although the topology and volume of the two molecules are very similar, the difference in bilayer thickness, d , and the area per lipid, A , are significant. For PSM, $d =$

(4.34 ± 0.05) nm, and $A = (0.52 \pm 0.01)$ nm², but for DPPC, $d = (3.58 \pm 0.05)$ nm, and $A = (0.65 \pm 0.01)$ nm². The observations are in agreement with experimental values: the area per lipid for SM in l_d phase has been shown to vary between 0.47 and 0.55 nm² [Maulik and Shipley, 1996; Li et al., 2000], whereas for DPPC the area is 0.64 nm² [Nagle and Tristram-Nagle, 2000].

As the values for the area per lipid vary, and there are experimental difficulties in determining this value [Nagle and Tristram-Nagle, 2000], more reliable conclusions about packing may be determined on the basis of acyl chain order parameters, as represented in Figure 3.1. It is evident from the graphs that the acyl chains of PSM are much more ordered than the ones of DPPC. For comparison, all existing NMR studies suggest significantly higher ordering of the acyl chains [Neuringer et al., 1979; Mehnert et al., 2006] and of the headgroups [Siminovitch and Jeffrey, 1981] in SM than in PC bilayers. Also, in binary SM-PC mixtures, the addition of SM has been shown to increase the overall order of the system [Guo et al., 2002; Steinbauer et al., 2003].

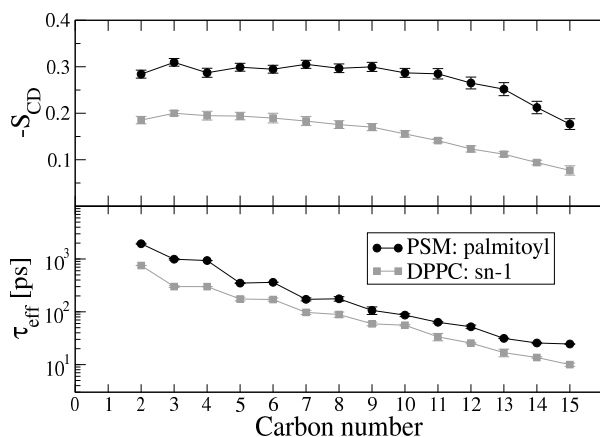


Figure 3.1: The deuterium order parameters (top) and the effective rotational autocorrelation times of the CH-vectors (bottom) in PSM and DPPC bilayers. The carbon numbering is as in Figure 1.2.

It is interesting to note from Figure 3.1 that it is not only the order of the chains that has increased in the PSM bilayer, but also the rotational dynamics of the chains has significantly slowed down, as characterised by the characteristic decay time of the rotational autocorrelation function of the C-H bonds. The rotational dynamics is related to the spin-lattice relaxation time in the NMR experiment as introduced in the previous sections. However, the spin-lattice measurements are lacking for SM.

Other dynamic features of the lipids, such as lateral diffusion and overall rotational motions of the lipids are also significantly slowed down in the PSM bilayer when compared to DPPC. For example, the lateral diffusion coefficient is $D_T = (0.38 \pm 0.03) \times 10^{-7}$ cm²/s for PSM and $D_T = (1.27 \pm$

$0.03) \times 10^{-7} \text{ cm}^2/\text{s}$ for DPPC. The timescale of the overall rotations of the lipids around their main axis is slowed down from around 1.0 ns (DPPC) to 6.9 ns (PSM).

3.3 Hydrogen Bonding

Increased packing of lipids means decreased entropy and thus involves a cost of free energy. As the only practical difference in the molecular structures of PSM and DPPC are the hydroxyl and amide groups of PSM that are lacking in DPPC, the free energy cost of packing in SM must be paid by the energy of interaction of these groups with the rest of the system and/or with each other. In practice, as the two groups contain polar hydrogens, this means hydrogen bonding. The features of hydrogen bonds in the studied bilayers and how to analyse them in a classical simulation are discussed below.

Although a classical simulation fails to include quantum effects such as polarisation, classical two-body potentials have been shown to predict the correct qualitative static and dynamic features of hydrogen bonding liquids such as water [Ladanyi and Skaf, 1993]. Thus, with a careful choice of parameters in a classical simulation, it is possible to make conclusions about the occurrences and lifetimes of hydrogen bonds within and between biomolecules.

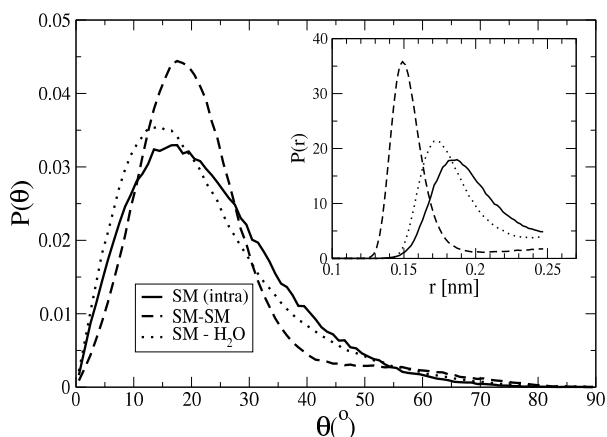


Figure 3.2: Angular distributions and hydrogen-acceptor distance distributions (inset) of various hydrogen bonding types within the PSM bilayer.

A hydrogen bond is formed by two electronegative atoms, a donor (D) and an acceptor (A), with a hydrogen (H) attached covalently to the donor. To define the conformation of a hydrogen bond, one generally uses either energetic [Sciortino et al., 1990] or geometric [Luzar and Chandler, 1996] criteria. In this work, we have utilised a geometric criterion for the hydrogen-acceptor distance d_{HA} and the donor-hydrogen-acceptor angle θ_{DHA} . By

plotting the distributions for the distance and the angle of selected D-A pairs, one may judge whether any hydrogen bonds occurred during the simulation. The distributions in Figure 3.2 justify the choice for the criteria $d_{\text{HA}} \leq 0.25 \text{ nm}$ and $\theta_{\text{DHA}} \leq 90^\circ$, so that all necessary hydrogen bond types are captured in the analysis.

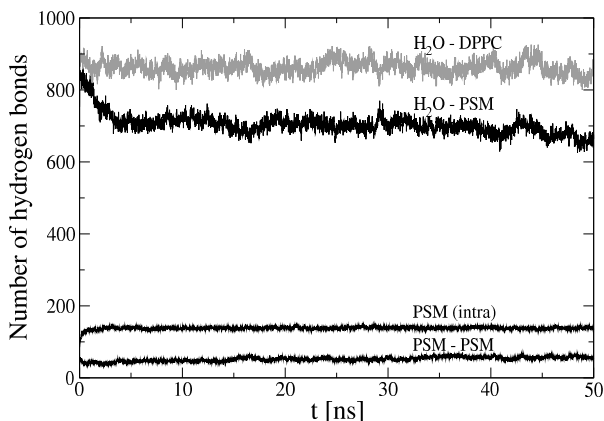


Figure 3.3: Average number of hydrogen bonds as a function of time in the DPPC and PSM bilayer systems.

Figure 3.3 reveals the number of hydrogen bonds between different molecular groups as a function of simulation time. It is easy to see that after a few nanoseconds, the total number of hydrogen bonds in the system finds an equilibrium and starts to fluctuate around a constant value: during any time interval the same average number of new bonds are formed as old bonds are broken. The situation becomes interesting when one compares the average numbers of hydrogen bonds in different kinds of systems at equilibrium. For example, Figure 3.3 reveals that DPPC forms more bonds with water than PSM. On the other hand, DPPC lacks hydrogen bond donors, which makes it impossible for hydrogen bonds to occur between DPPC molecules or intramolecularly within DPPC molecules. This is not the case for PSM, which means that a network of hydrogen bonds is formed *within* the PSM-bilayer, not just between lipids and water. This leads to major implications on the properties of the bilayer, as discussed in the previous section.

To further characterise the hydrogen bonding characteristics within a PSM bilayer, it is useful to look at the different functional groups separately. The hydroxyl group is mostly (91%) involved with *intramolecular* hydrogen bonds with the phosphate oxygens. After being formed, these bonds are very stable, lasting on average longer than the simulation. The NH-group, on the other hand, is mostly involved with the *intermolecular* bonds, mainly bonding with the hydroxyl oxygen (63%) and the carbonyl oxygen (21%). The breaking/reforming timescale of the intermolecular bonds are typically

in the order of 1-7 ns. Water makes hydrogen bonds with all polar groups of the lipids, but mostly with the phosphate oxygens of PSM and DPPC, the timescale of the bond breaking/reforming being typically in the order of 10 ps.

3.4 Effects of Chain Length and Saturation

Sphingomyelins of biological membranes constitute a variety of molecular species with varying chain length and degree of unsaturation. To better understand the origins of this variety, it is useful to study systematically the factors affecting the properties of SM bilayers. Figure 3.4 summarises the results on bilayer dimensions when one of the chains of SM (acyl chain) has been varied between 16 and 24 carbons in length, and when the unsaturation has been varied between full saturation and monounsaturation.

The graphs reveal two aspects. First, for all chain lengths unsaturation increases the area per lipid significantly when compared with saturated SM. A single double bond in one of the chains can therefore drastically alter the overall fluidity of the bilayer, which in turn is reflected in almost all other properties of the bilayer. The effect of chain length on the area per lipid is much less clear. There seems to be a slight trend of decreasing area per lipid with increasing chain length, but the effect is less significant than unsaturation.

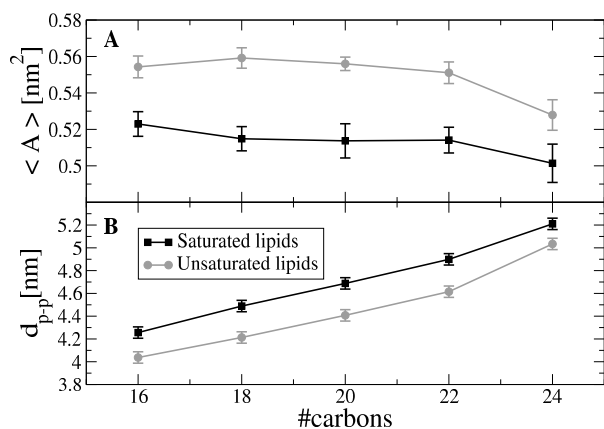


Figure 3.4: Average structural quantities of SM bilayers as a function of acyl chain length: area per lipid (top), and the bilayer thickness (bottom). Separate graphs have been drawn for the saturated lipids and for the monounsaturated ones.

The most prominent effect of chain length is reflected on the bilayer thickness, which increases linearly with chain length. It has been proposed that the match between the hydrophobic length of an integral protein and the hydrophobic thickness of the membrane could be important for the partitioning

of the protein into different membrane environments [Jensen and Mouritsen, 2004; Andersen and Koeppe, 2007]. From this point of view, the high variety of chain lengths of SM may be understood as being important for the cells, as they need to adjust the hydrophobic thickness of their membranes and regulate the partitioning of the membrane proteins.

The effect of double bonds and the chain length on the ordering and the dynamics of the chains themselves is summarised in Figure 3.5. The order parameter profiles show that the double bond causes a large peak locally in the chain order, but has almost negligible effects close to the chain ends. As for the chain dynamics, the τ_{eff} profiles also display a local effect in the vicinity of the double bond. A natural conclusion from this is that the effect of unsaturation is local and that the unsaturation most probably increases the area per lipid through local changes in lateral pressure [Ollila et al., 2007].

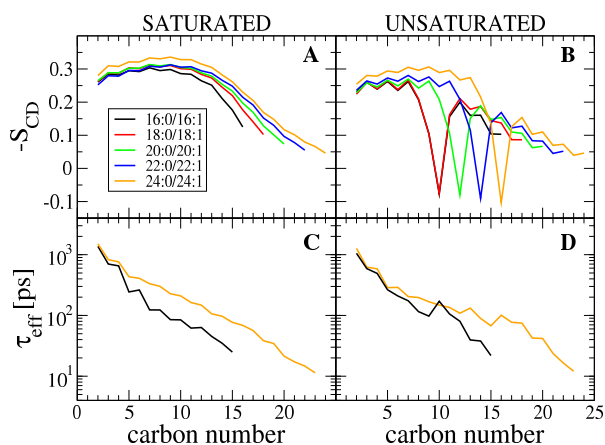


Figure 3.5: Deuterium order parameters (top panels), and the effective decay times of the rotational autocorrelation functions of C-H bonds (bottom) as a function of the carbon position along the chain in SM bilayer systems. Separate graphs have been shown for the amide-linked acyl chain in the different systems (see legend for details). Only two systems have been shown in each of the bottom panels for clarity.

The effect of chain length on the ordering and dynamics of the chain is much less significant. The long unsaturated chains are somewhat more ordered and their rotational dynamics is slower than that of the short ones, but the effect is small. Also, the chain ends in the middle of the bilayer are somewhat less ordered for long chains than for the short chains.

3.5 Interdigitation

A highly interesting phenomenon is the interaction of the opposite monolayers through the bilayer centre. This interaction is mediated by the interdigitation of acyl chains of the lipids and is possibly related to information transfer across the membrane. As SMs typically have long chains, and a relatively large chain length disparity, they make good candidates for studying the phenomenon of interdigitation. Especially in the gel phase, but also to some extent in the fluid phase, the long chains have been suggested to interdigitate through the bilayer centre and reach far to the opposite side of the bilayer. This effect has been seen also in our simulations, see for example the snapshot in Figure 3.6. Recently, it was proposed that interdigitation could cause co-localization of lipid domains in bilayers that display phase separation [Allender and Schick, 2006].

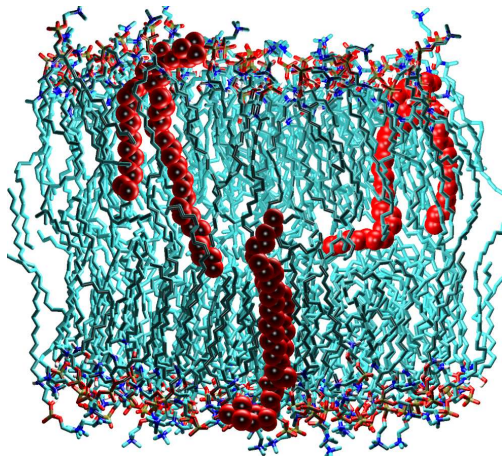


Figure 3.6: Snapshot from the simulation of 24:1-SM bilayer. A few molecules have been rendered differently to highlight the different molecular conformations and interdigitation through the bilayer centre.

Interdigitation was first suggested on the basis of electron density graphs, measured by x-ray diffraction. These graphs showed a density peak in the middle of the bilayer instead of a trough, which is typical for lipids with chains of similar length. Using our model, we were able to reproduce this density peak for SMs (Figure 3.7) and compare the profiles with the ones from x-ray diffraction [Maulik et al., 1986]. A more detailed analysis led to the conclusion that the peak is indeed caused by the increased packing of the ends of the long chains in the middle of the bilayer.

Two effects are observed from the two lower panels of Figure 3.7: the longer chains reach further towards the opposite monolayer, but on the other hand, there is a significant contribution from chains that have been bent. Therefore, it is difficult to quantify the extent of interdigitation in the studied

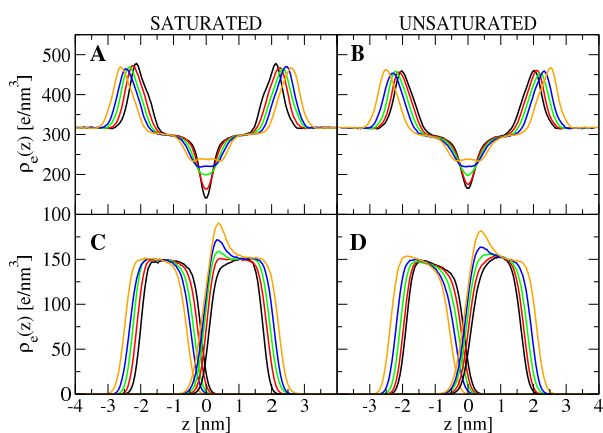


Figure 3.7: Electron densities across the whole simulated system (top) and for the sphingosine, and the acyl chains of the opposite monolayers separately (bottom) of the simulated SM bilayer systems. For colour coding, see Figure 3.5.

systems and the possible biological significance of the observation. A possibility to give more quantitative arguments about the significance of interdigitation would be to conduct non-equilibrium simulations and to measure the interlayer friction for varying systems [Shkulipa et al., 2005]. Work in this direction is underway.

Properties of Sterols

4.1 Motivation

The various effects of sterols on membrane properties are mainly explained by the fact that the sterols accommodate themselves into the hydrophobic region, reducing the free volume and increasing the order of the neighbouring acyl chains. At high enough sterol concentration, the overall properties like elasticity of the membrane are altered, and particularly in the case of cholesterol, the l_o phase is formed. Also, in ternary mixtures of lipids such as SM, CHOL, and PC, a phase separation of the l_o and l_d regions is observed, which is possibly related to the lipid rafts of biological membranes.

However, the nature of molecular interactions between SM, CHOL, and PC is not fully understood. A common interpretation is that a "specific" interaction such as hydrogen bonding between SM and CHOL leads to strong attraction between these two molecules [Sankaram and Thompson, 1990; Li et al., 2001; Simons and Vaz, 2004]. On the other hand, other studies suggest that no specific hydrogen bonding is needed and that the hydrophobic interactions might play a more important role under given conditions [Slotte, 1999; Holopainen et al., 2004].

A closely related issue is the factors that determine the extent of how CHOL increases the acyl chain order. In the hydrophobic region, the van der Waals interactions dominate, but a second contribution comes from the electrostatic interactions of the headgroup of CHOL with the polar parts of other lipids and with water.

In this chapter, different mechanisms of molecular interactions between sterols and other lipids are reviewed and the key results from the simulation studies in *Paper III* and *Paper IV* are presented. In particular, we study the molecular interactions in a system with dilute CHOL and SM concentrations, embedded in a POPC matrix. Finally, the ordering capacity of CHOL is compared to that of other sterols.

4.2 Ordering Capacity of Cholesterol

First, to understand the capacity of cholesterol to order the acyl chains of neighbouring lipids, let us examine Figure 4.1. The figure shows the S_{CD} order parameters of the saturated palmitoyl chains in both lipids in two situations: when the lipid has a cholesterol neighbour, and when it has none (i.e. it has only POPC neighbours). The figure reveals clearly that, throughout the chain length, CHOL increases the order of the acyl chain of both types of neighbouring lipids. This conclusion is in agreement with a previous study, which showed that CHOL has a tendency to order the neighbouring acyl chains within a radius of a few nanometres [Pitman et al., 2004].

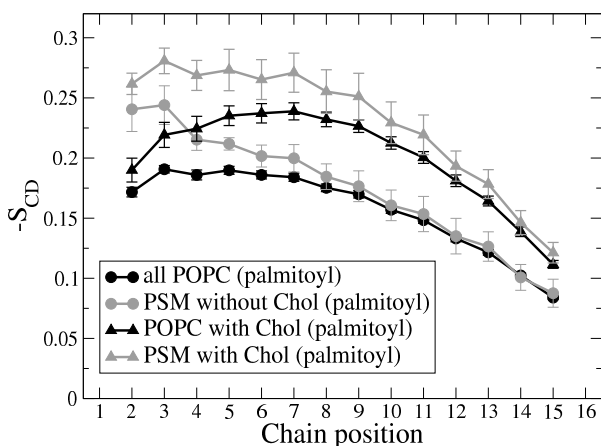


Figure 4.1: The deuterium order parameters of PSM and POPC, plotted separately for those lipids that are either neighbours or non-neighbours of CHOL.

Another clear conclusion from Figure 4.1 is that CHOL increases the ordering of PSM more than that of POPC. On average, the order parameter in POPC changes by 0.041 but in PSM by 0.066. This is an indication of the different nature of the PSM-CHOL interaction when compared to the POPC-CHOL interaction. Here one should note that the difference must be due to local lipid-lipid interactions, because the overall membrane environ-

ment, dictated by the excess POPC matrix, may be assumed to be similar for each of the separate CHOL molecules in the system.

Another aspect of CHOL order may be found in Figure 4.2, which presents the tilt of cholesterol molecules with respect to the bilayer normal in two different situations: when surrounded only by POPC molecules, and second, when one of the neighbours is PSM. The graphs reveal that having a PSM neighbour induces a significantly less tilted orientation of CHOL with respect to the bilayer normal. Clearly, the close neighbourhood of PSM increases the order of CHOL – an indication of a specific interaction between these molecules.

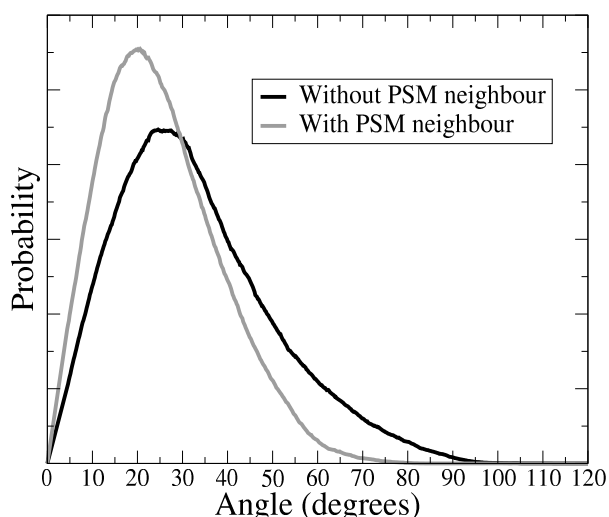


Figure 4.2: The angular distribution of the ring structure of CHOL with respect to the bilayer normal, plotted separately for those CHOL molecules that have a PSM neighbour and those that do not.

The high ordering capacity of cholesterol is usually related to the attractive van der Waals interactions between the hydrophobic parts of CHOL and the acyl chains. For example, saturated chains have been shown to favour the smooth α -face of CHOL instead of the rougher β -face [Pandit et al., 2004a; Róg and Pasenkiewicz-Gierula, 2006a]. The results in *Paper IV* support this idea. We find that the saturated chains of POPC and PSM are on average more ordered when next to the α -face of CHOL than the β -face, whereas the unsaturated chain of POPC shows no such difference. The differential ordering of the acyl chains on the two sides of CHOL possibly also explains the observed preference of PSM for the α -face.

Here one should note that the electrostatic interactions of CHOL's head-group with the rest of the system probably play an additional role in regulating the tilt of CHOL, which then again is reflected in the order of the neighbouring acyl chains. The situation is complex with many competing

effects taking place simultaneously, and it is difficult to estimate the relative significance of the different contributions. However, the next sections will discuss aspects of the phospholipid interactions with the CHOL headgroup.

4.3 Direct Hydrogen Bonding

The hydrogen bonding characteristics between different molecules in the system studied in *Paper IV* are summarised in Table 4.1. Perhaps the most notable effect is the nearly complete lack of direct hydrogen bonds between CHOL and PSM. Considering the much higher number of direct bonds between other molecular pairs such as CHOL-POPC and PSM-POPC, it seems evident that direct hydrogen bonding can not be the principal interaction that would lead to molecular attraction between PSM and CHOL within a PC matrix, at least at low CHOL/PSM concentrations.

Table 4.1: Average numbers of hydrogen bonds per corresponding pair for different molecules.

	POPC	PSM	Water
POPC	—	0.93	6.99
PSM without Chol	0.93	1.08 ¹	6.39
PSM with Chol	0.93	1.12 ¹	6.2
Chol without PSM	0.88	—	0.54
Chol with PSM	0.82	0.08	0.44

¹PSM intramolecular H-bonds, involving the OH-group.

Hints of other interesting phenomena can be found after a more detailed comparison of the numbers in Table 4.1. For example, the hydrogen bonding of CHOL with water is diminished when it has a PSM neighbour, and on the other hand, the number of intramolecular bonds of a PSM is increased when it has a CHOL neighbour. It seems as if the hydrogen bonding patterns of these two molecules are altered when they are next to each other, even though no direct hydrogen bonding is observed.

It is worthwhile to consider the possible effect of the employed force field on the conclusions on hydrogen bonding. Simulation studies on SM bilayers with different force field parametrisations [Chiu et al., 2003; Hyvönen and Kovanen, 2003; Mombelli et al., 2003] have yielded very similar hydrogen bonding patterns as the model used in this work (see Section 3.3). Also, studies on binary SM-CHOL mixtures have produced results with significant direct hydrogen bonding [Khelashvili and Scott, 2004; Róg and Pasenkiewicz-Gierula, 2006b], mainly between the amide group of SM and the head group

of CHOL, but to some extent with the hydroxyl groups. However, previous studies of ternary PC-SM-CHOL mixtures [Pandit et al., 2004a,b] have not reported any direct hydrogen bonds between SM and CHOL either. It is not completely clear, how sensitive the results are for example to changes in force field parameters such as partial charges. It is possible that the interactions overall in this field are somewhat off balance and for example the lowering of the partial charges of the carbonyl oxygens in PC would change the hydrogen bonding pattern. Another possibility is that the current force field and the current conclusions are right. More detailed computational work is needed in order to evaluate and possibly improve the force fields. Also clever experiments are called for, in order to validate the predictions made with the current models.

4.4 Head Group Interactions

In addition to hydrogen bonds, other electrostatic interactions play a role in lipid-lipid interactions. For example, the PC-headgroup has a negatively charged phosphate (P) and a positively charged choline (C) group. The interactions between a set of PC-headgroups are understood in terms of a dipole-dipole interaction, which is either attractive or repulsive depending on the relative orientations of the dipoles. Even though the PC-headgroup is incapable of forming hydrogen bonds, a net attractive electrostatic interaction is possible with the OH-group of CHOL and the positively charged choline. A snapshot showing the typical conformation that involves this interaction is in Figure 4.3.

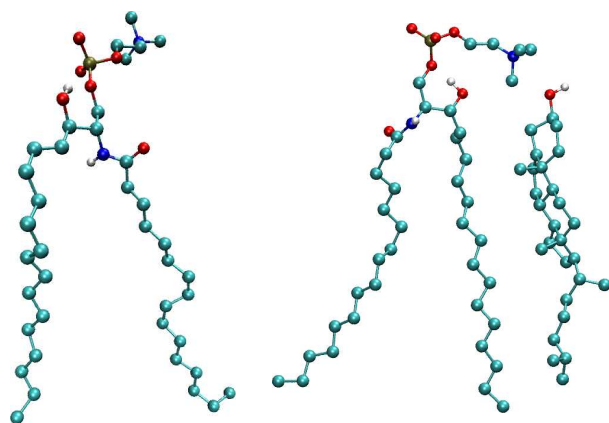


Figure 4.3: Snapshots representing typical PSM orientations, for a PSM without CHOL neighbour (left) and a PSM with CHOL neighbour (right).

In *Paper IV* it was shown that even though PSM seems "reluctant" to form direct hydrogen bonds with CHOL, the charge-pairs between its headgroup

and CHOL are relatively much more abundant than those between POPC and CHOL. To characterise this somewhat surprising effect in greater detail, all POPC and PSM lipids in this study were divided into two groups: those which have a CHOL neighbour and those which do not. The distributions of the headgroup orientations (characterised by the P-N vector) with respect to bilayer normal in the two cases are plotted in Figure 4.4.

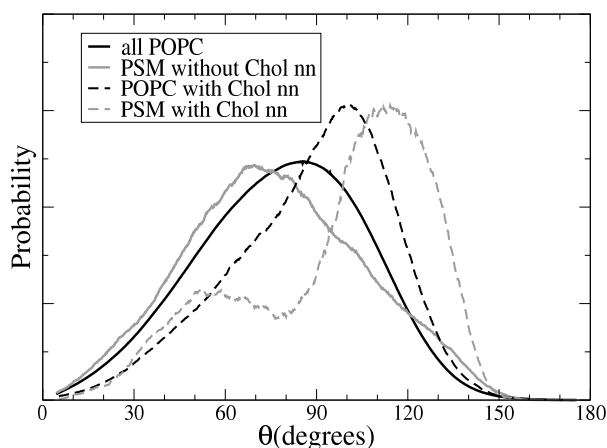


Figure 4.4: Angular distribution of the headgroup P-N vector with respect to the bilayer normal. Plotted separately for those PSM or POPC molecules that are either neighbours of CHOL or for those that are not.

The graphs in Figure 4.4 reveal that without a CHOL neighbour, the headgroup of POPC is tilted somewhat more towards the bilayer centre than the headgroup of PSM. The neighbourhood of CHOL makes an interesting difference, however. While the tilt of POPC's headgroup changes only slightly, the headgroup of PSM becomes more tilted towards the bilayer centre than the one of POPC. At the same time, the distribution of the headgroup angles becomes bimodal for PSM. An analysis of the hydrogen bonding patterns hints that the intramolecular hydrogen bonding of PSM might help in stabilising the bending of the PSM's headgroup downwards and thus further the charge-pair interaction between PSM and CHOL. The idea is illustrated in the two snapshots of Figure 4.3.

Another related interaction is the so-called umbrella effect [Huang and Feigenson, 1999], which is probably enhanced by the charge-pairing interaction. The idea of the umbrella effect is based on the fact that CHOL is largely hydrophobic and benefits when shielded from water by other headgroups. In a more detailed analysis in *Paper IV*, we find that the hydrophobic parts of CHOL indeed have less overlap with water when charge-paired with PSM than when charge paired with POPC. Based on this observation, it was proposed that the combination of charge-pairing and hydrophobic effects could be more important for PSM-CHOL interaction than direct hydrogen bonding, but estimating the relative strengths of the various effects is difficult.

The issue remains to be fully solved by either much more detailed free-energy calculations or detailed experiments.

4.5 Sterol Tilt vs. Fluidity

The previous sections showed that PSM's acyl chains are more ordered when next to CHOL. On the other hand, the body of CHOL was less tilted when next to PSM. Figure 4.5 shows that the order parameters of the chains of PSM and POPC are strongly correlated with the tilt angle of a neighbouring CHOL. Higher instantaneous tilt of CHOL weakens the order of the neighbouring acyl chains.

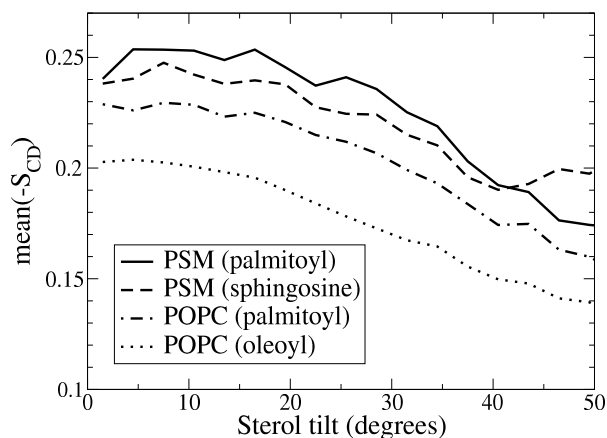


Figure 4.5: Order parameter of acyl chains that are neighbours of CHOL, plotted as a function of CHOL's tilt angle.

In a more detailed analysis, the effect of Figure 4.5 was found to split into two contributions. First, an increased tilt of cholesterol increases the *gauche/trans* fraction of the dihedral angles in a neighbouring chain, which is reflected in a decrease in the order parameter values. On the other hand, a more tilted CHOL also increases the overall tilt of the neighbouring acyl chains, causing an additional decrease of the order parameters. In Figure 4.5, both of these effects are lumped together into a single order parameter value. However, the value of S_{CD} is highly useful as it is experimentally measurable and as it correlates with a number of macroscopic properties of bilayers [Bloom et al., 1991].

Concluding, a strong correlation between the instantaneous tilt of CHOL and the order parameters of the neighbouring acyl chains suggests that either one of the two can be measured to give similar information. For bilayers with dilute CHOL concentrations, measuring the distribution of CHOL tilt gives

information about the local lipid environment around the CHOL molecules. At higher concentrations, the measured average tilt would be more and more related to the average order of the whole system.

4.6 Comparison of Sterols

The above discussion shows that CHOL has a strong tendency to increase the order of the neighbouring acyl chains. This property is one of the key factors leading to the formation of the l_o phase and, under certain conditions, the formation of phase-separation and lipid rafts. Previous computational studies have indicated that even minor modifications in the molecular structure of CHOL weaken the ordering properties and/or alter the partitioning of CHOL [Vainio et al., 2006; Róg et al., 2007].

In *Paper III*, we compare the effects of four different sterols on membrane properties. For details of the different structures, see Figure 1.2. In addition to CHOL, we study two physiological analogs: ketosterol (polar part modified) and desmosterol (tail modified). Additionally, we include one artificial sterol (DCHOL), with the two methyl groups on the β -face deleted. The idea of the study was to examine how modifications of different parts affect the function of the sterols.

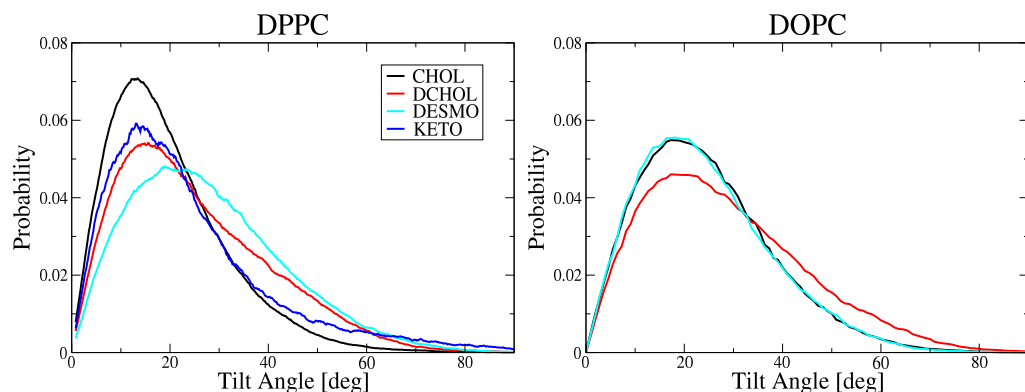


Figure 4.6: Sterol tilt angle distributions in DPPC (left) and DOPC (right) bilayers with respect to bilayer normal. In each case the sterol content is 20 mol-%.

Figure 4.6 shows the distribution of tilt angles of different sterols in binary mixtures with DPPC or DOPC. The first observation from the figure is that in the unsaturated DOPC-environment, all sterols but desmosterol display

higher tilts than in the saturated DPPC environment. Moreover, the differences between the effects of different sterols in saturated membranes are much larger than in unsaturated membranes. Actually, CHOL and desmosterol behave exactly similarly in the DOPC-environment, as supported also by experiments [Huster et al., 2005]. However, none of the sterols is better than CHOL in terms of ordering properties in any environment. In particular, CHOL has a significantly lower tilt in the saturated DPPC bilayer when compared with any of the other sterols.

In *Paper III*, we find that the correlation between sterol tilt and the average order parameters of the acyl chains holds for all studied systems. Therefore, concluding from Figure 4.6, CHOL seems to be superior in increasing the order of saturated acyl chains. This general conclusion is in accord with previous studies that have been carried out to resolve the effect of different sterols on membranes [Korstanje et al., 1990; Urbina et al., 1995; Vainio et al., 2006]. As CHOL is the most abundant sterol in most eukaryotic membranes, it is natural to assume that the ordering capacity is directly linked to the biological function.

The interesting case of ergosterol has not been included in this work. Previous studies have shown that ergosterol is even more effective in increasing the order of saturated acyl chains than CHOL [Urbina et al., 1995; Czub and Baginski, 2006; Cournia et al., 2007]. It has been proposed that the main cause for this are the additional methyl group and the double bond of the side-chain of ergosterol, which restrict the conformational freedom and mobility and lead to more effective packing [Czub and Baginski, 2006]. Additional studies would be needed to completely understand the interplay between sterol structure and functions. An intriguing question about a possibility to create a synthetic molecule that would beat the properties of natural sterols remains to be answered. However, the next chapter concentrates on bilayers with CHOL and considers the properties of lipid raft membranes.

Lipid Raft Simulations

5.1 Motivation

Various experiments have displayed the coexistence of l_o and l_d domains in model membranes under certain conditions, but no direct evidence exists of the exact nature of domains in membranes of living cells. Properties of rafts, such as their characteristic sizes, lipid composition and lifetimes have remained unclear. Even results discussing the nature of the lipid phases in experimental model membranes vary [Clarke et al., 2006; Mehnert et al., 2006]. As the smallest estimates for the sizes of rafts are in the order of nanometres, they could in principle be assessed by atom-scale simulation. It is perhaps surprising that only a few simulation studies [Pandit et al., 2004a,b] have been carried out on ternary mixtures of CHOL, SM, and PC.

This chapter discusses the simulation results on lipid raft membranes, presented in *Paper V*. First, the most important average properties of raft and non-raft membranes are summarised and discussed. Then, details of calculating the bending rigidity, the area compressibility, and the lateral pressure profiles of each of the membranes are reviewed in separate sections. Finally, the possible biological consequences of the findings are discussed through their effects on membrane proteins.

5.2 Overview of Membrane Properties

Average properties of the simulated raft and non-raft membranes are summarised in Table 5.1. The first observation is the strongly condensed nature of the two raft membranes (with POPC:PSM:CHOL = 1:1:1 or 2:1:1). The decreased area per lipid, together with the increased bilayer thickness and order parameter values indicate that acyl chains in the raft-membranes are much more highly packed than in the non-raft system (with POPC:PSM:CHOL = 62:1:1). When looking at the area compressibility, K_A , and bending rigidity, k_c , values, it is evident that the raft systems are characterised by a much more rigid nature than the non-raft membrane. The lateral diffusion coefficients, D , reveal more than an order of magnitude slower dynamics in raft membranes when compared to non-raft membranes.

Table 5.1: Average structural and thermodynamic properties calculated from the simulations of systems S_A , S_B and S_C : average area per lipid (A), bilayer thickness (d), deuterium order parameter (S_{CD}) of acyl chain carbons 5-7, area compressibility modulus (K_A), bending rigidity modulus (k_c) and lateral diffusion coefficients (D).

System	S_A	S_B	S_C
POPC:PSM:CHOL	1:1:1	2:1:1	62:1:1
A [nm ²]	0.41 ± 0.01	0.44 ± 0.01	0.66 ± 0.01
d [nm]	4.40 ± 0.05	4.29 ± 0.05	3.53 ± 0.05
- S_{CD} (5-7)	0.41	0.36	0.18
K_A [10 ⁻³ N/m]	2700 ± 700	1000 ± 400	200 ± 100
k_c [10 ⁻²⁰ J]	10 ± 2	7 ± 2	6 ± 2
D_{popc} [10 ⁻⁷ cm ² /s]	0.037 ± 0.002	0.08 ± 0.02	0.67 ± 0.06
D_{psm} [10 ⁻⁷ cm ² /s]	0.036 ± 0.002	0.07 ± 0.02	0.8 ± 0.2
D_{chol} [10 ⁻⁷ cm ² /s]	0.038 ± 0.002	0.08 ± 0.02	0.5 ± 0.2

According to the experimental phase diagram represented in Figure 1.4, our simulations of raft membranes should display a coexistence of l_d and l_o phases, while the non-raft membrane should be in the l_d phase. Considering the unexpectedly slow diffusion within these two membranes, it becomes evident that the simulation time of 100 ns is too small to cover complete mixing of the lipids and allow the formation of domains. However, our analysis shows that the lipids move on average approximately over their own size within the simulation time scale, and that the local interactions between the neighbouring lipids are adequately sampled. This justifies the assumption that the average bulk properties of the studied membranes do arise from the lipid-lipid interactions of their constituents.

Recent experimental results give further support for our choice of systems. First, an AFM study reported a thickness difference of 0.6 – 0.9 nm in a bilayer that displayed a phase coexistence of the l_d and l_o domains [Rinia et al., 2001]. This is in agreement with the thickness of the simulated bilayers. Another is a pulsed-field NMR study [Filippov et al., 2006], which reported two populations of diffusion coefficients in DOPC-SM-CHOL mixtures with 10–30 mol% CHOL at 300 K, one corresponding to the l_d phase ($D \approx 1 \times 10^{-7} \text{ cm}^2/\text{s}$) and the other to the l_o phase ($D \approx 1 \times 10^{-8} \text{ cm}^2/\text{s}$). The agreement of these two results supports the idea that two of the simulated bilayers are representatives of the environment within a l_o domain of these studies, whereas one of the systems is in the l_d domain.

The bilayer dimensions, A and d , of the non-raft bilayer are in agreement with previous findings on pure POPC bilayers in the l_d phase [Kučerka et al., 2005; Patra et al., 2006]. Also, the area compressibility modulus, K_A , and the bending rigidity, k_c are in line with previous studies of pure PC bilayers, reporting $K_A = 140 - 300 \times 10^{-3} \text{ N/m}$ and $k_c = 4 - 9 \times 10^{-20} \text{ J}$ [Evans and Rawicz, 1990; Lindahl and Edholm, 2000a; Rawicz et al., 2000].

The two lipid raft simulations may be compared with binary PC-CHOL systems with similar CHOL concentrations. Comparison with previous studies shows that the values for A in Table 5.1 for S_A and S_B are 0.1 to 0.4 nm² lower than expected for binary PC-CHOL systems with similar CHOL concentrations [Hofsäss et al., 2003; Falck et al., 2004]. Also, we find higher differences in K_A values than previous reports, predicting maximally 5–7 fold increases in the K_A values upon CHOL addition into PC bilayers [Needham et al., 1988; Hofsäss et al., 2003]. Particularly interesting is the study reporting a much higher value of $K_A = 1718 \times 10^{-3} \text{ N/m}$ for a SM-CHOL bilayer than the value of $K_A = 781 \times 10^{-3} \text{ N/m}$ for a PC-CHOL bilayer, both with 50 mol% CHOL [Needham and Nunn, 1990]. Concluding, the above values suggest an additional role of PSM in ordering and rigidifying the bilayer. This is possibly related to the additional intermolecular hydrogen bonds induced by PSM.

5.3 Undulations and Bending Rigidity

Let us consider a nearly planar membrane, whose height over the xy -plane (projected area A_p) is described by the function $h(x, y)$. For an example, see Figure 5.1.

By definition, the curvature is given by $H = \nabla^2 h$. Additionally in the small gradient approximation, the local stretch of membrane area due to undu-

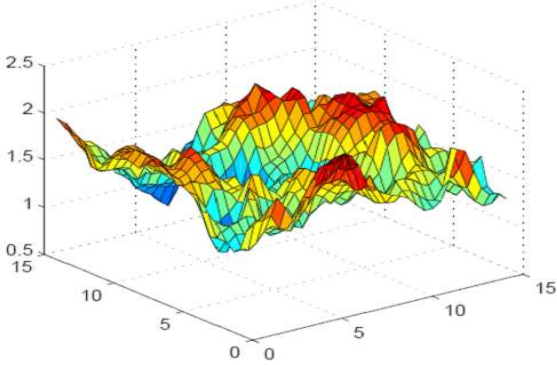


Figure 5.1: An example of a fitted surface to an undulating membrane.

lation is $(1/2)\gamma(\nabla h)^2$ [Safran, 1994]. After neglecting the terms related to spontaneous and Gaussian curvatures in the Helfrich formulation of equation 2.21, the free energy reads:

$$F_{bend} = \int_{A_p} dx dy \left[\frac{1}{2} k_c (\nabla^2 h(x, y))^2 + \frac{1}{2} \gamma (\nabla h(x, y))^2 \right]. \quad (5.1)$$

From a bilayer simulation, it is possible to estimate the function $h(x, y)$ by fitting a grid onto the lipid/water interfaces of the two monolayers separately to yield functions h_1 and h_2 [Lindahl and Edholm, 2000b]. The average of the two layers then gives $h(x, y) = 0.5[h_1(x, y) + h_2(x, y)]$, as shown for example in Figure 5.1. The periodic boundary conditions used in a simulation lead to a convenient representation after a discrete Fourier transform:

$$F_{bend} = A_p \sum_{\vec{q}} |h_{\vec{q}}|^2 \left[\frac{1}{2} k_c q^4 + \frac{1}{2} \gamma q^2 \right]. \quad (5.2)$$

Applying the equipartition theorem to the above equation yields $k_B T/2$ average energy per each independent term in the sum. This immediately gives us the undulation spectrum:

$$\langle |h_{\vec{q}}|^2 \rangle = \frac{k_B T}{A_p (k_c q^4 + \gamma q^2)}. \quad (5.3)$$

For small q -vectors ($q < q_0 = \sqrt{\gamma/k_c}$), the spectrum is dominated by the bending rigidity term, and the k_c value can be estimated by fitting an approximate form $\langle |h_{\vec{q}}|^2 \rangle \sim q^{-4}$. On the other hand, the sum over all wave

vectors in equation 5.3 can be evaluated explicitly to yield the mean squared undulation amplitude of the whole membrane:

$$\langle h^2 \rangle = \sum_{\vec{q}} \langle |h_{\vec{q}}|^2 \rangle \approx \frac{k_B T A}{8.3\pi^3 k_c}. \quad (5.4)$$

The above described undulatory behaviour involves correlated motions of the two monolayers of a membrane. Another aspect would be to study the peristaltic motions of the membrane through monitoring the thickness oscillations by the function $d(x, y) = h_2(x, y) - h_1(x, y)$. To a first approximation, the free energy related to peristaltic motions is a sum of the bending rigidity (described by k_d) and a harmonic term (k_e) that restores the membrane thickness to its equilibrium value d_0 [Lindahl and Edholm, 2000b]:

$$F_{per} = \int_{A_p} dx dy \left[\frac{1}{2} k_d (\nabla^2 d(x, y))^2 + \frac{1}{2} k_e (d(x, y) - d_0)^2 \right]. \quad (5.5)$$

Now, a similar treatment as for undulations yields the peristaltic spectrum:

$$\langle |h_{\vec{q}}|^2 \rangle = \frac{k_B T}{A_p (k_d q^4 + k_e)}. \quad (5.6)$$

The major difference of the peristaltic spectrum when compared with the undulatory spectrum in equation 5.3 is that the undulatory spectrum reaches asymptotically a constant value when q decreases, whereas the undulations always increase when the system size is increased (q decreased). This effect is clearly seen in Figure 5.2 towards small q values.

The bending rigidity may be extracted from the undulatory spectra in Figure 5.2A either by fitting a function $\langle |h_{\vec{q}}|^2 \rangle \sim q^{-4}$ as discussed above or by calculating the sum of equation 5.4. Although the fitting is subject to large error due to the small number of points at the small- q area, the two methods yield very similar results as seen in Figure 5.2A.

It is interesting to see that the increasing content of SM and CHOL in the bilayer increase the bending rigidity values significantly. In *Paper V* we discuss these values and find an agreement with experimental studies. What is also interesting in Figure 5.2, is the observation that the large-scale (low- q) peristaltic wave modes are suppressed relatively much more than the undulatory modes in the raft-like membranes. This is understandable, as particularly CHOL has been found to accommodate the voids within

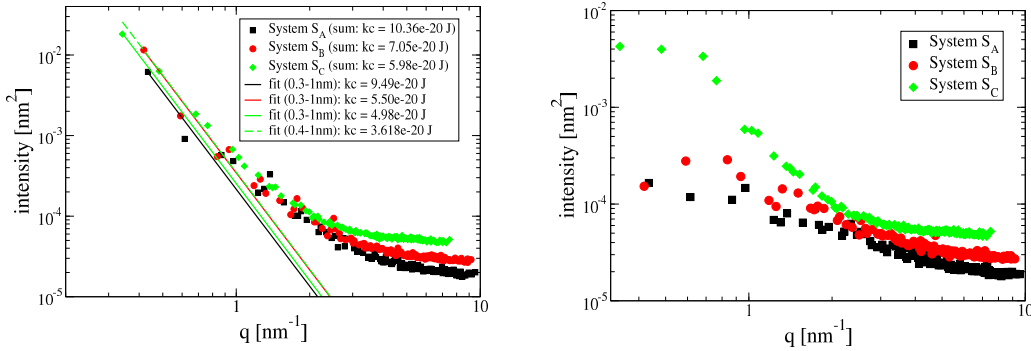


Figure 5.2: Undulatory (left) and peristaltic (right) spectral intensities per wave mode versus wave vector magnitude for the two raft systems and one non-raft system.

the membrane [Falck et al., 2004] and thus probably decrease the volume fluctuations involved with peristaltic motions. The observations related to peristaltic motions are much more difficult to compare with experiment and are, therefore, yet a less verified but novel prediction from the simulation.

One more thing to note is that all of the above discussion holds only for small enough q -values, or large enough length-scales. Typically the critical length scale is given by the average membrane thickness l_{cr} , such that $q_{cr} = 2\pi/l_{cr}$. In our work we have used $q_{cr} = 1.0 \text{ nm}^{-1}$. For very small length scales it is the protrusions of single lipids that dominate the spectrum. Relating a microscopic surface tension, γ_p to the free energy cost of protrusions, one yields a spectrum of the form:

$$\langle |h_{\vec{q}}|^2 \rangle = \frac{k_B T}{A_p (\gamma_p q^2)} \quad (5.7)$$

for the protrusions. Therefore, both spectra in Figure 5.2 should behave as q^{-2} at large q values because of the protrusions, and one should be able to find a value for γ_p by fitting. However, we found that different methods of fitting the grid (nearest neighbour, linear, cubic) lead to qualitatively different behaviour in this region of the spectrum and thus make it impossible to do the fitting. To properly evaluate protrusions, more elaborate analysis, such as height-height correlations of the neighbouring lipids should be conducted.

5.4 Area Compressibility

Here, one should note the effect of undulations on the measured K_A , as introduced in equation 2.23. First, the surface tension γ as presented in equation 5.1 is related to the local area stretch due to bending of the membrane. This is by definition different from the macroscopic surface tension, $\tilde{\gamma}$, measured over a large undulating membrane patch. Due to undulations, the true area of the membrane, A , is different from the measured area, A_p . The relation between the "bare" area compressibility modulus K_A and the measured one, \tilde{K}_A may be derived from [Marsh, 1997]:

$$\tilde{K}_A \approx K_A \left[\frac{1 - (k_B T A_p \tilde{\gamma} / 8\pi^3 k_c^2) / (\tilde{\gamma} A_p / \pi^2 k_c + 1)}{1 + (K_A k_B T A_p / 8\pi^3 k_c^2) / (\tilde{\gamma} A_p / \pi^2 k_c + 1)} \right]. \quad (5.8)$$

By setting $\tilde{\gamma} = 0$ and using the measured values of k_c , \tilde{K}_A and A_p for the largest and most fluid system in Table 5.1, we get a difference of about 0.2 % between the values of K_A and \tilde{K}_A . Thus, due to the small size of any realistic simulation box, we are practically always measuring the "bare" K_A , even with finite undulations.

5.5 Lateral Heterogeneity

We find two kinds of lateral heterogeneity in the studied systems. The first kind is prominent in the raft bilayers and seems to be related to the tendency of CHOL to order the neighbouring acyl chains. Figure 5.3 shows the average order acyl parameters for one of the raft simulations, plotted over the xy-plane and averaged over 10 ns. Comparison with the neighbouring plot for lateral density of cholesterol over the same time interval shows a clear correlation. The areas with higher lateral density of CHOL correspond to higher acyl chain order, whereas areas of depleted CHOL display higher disorder.

The other type of lateral heterogeneity is observed in the non-raft simulation and displayed in Figure 5.4. Here, the small concentration of CHOL seems insufficient to fully account for the observed large-scale lateral heterogeneity in chain order parameters. Instead, the regions of higher order seem to be related with the thickness fluctuations of the membrane. As can be seen from Figure 5.4, the more ordered regions are correlated with the thicker regions of the membrane and the less ordered regions with thinner regions. The idea is supported by the fact that the large scale peristaltic modes are

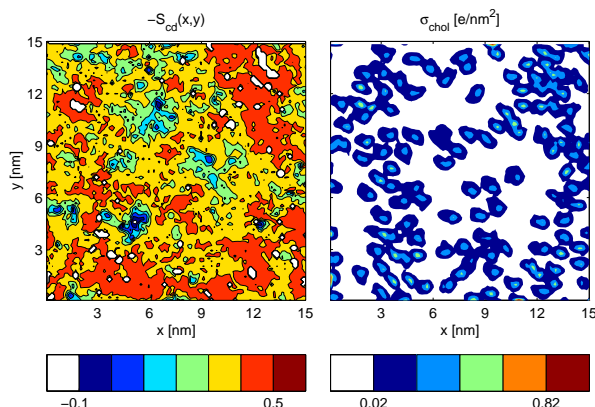


Figure 5.3: The deuterium order parameters of selected carbons (C5-C7) in POPC and PSM chains (left) and the CHOL density (right), binned in the xy -plane and averaged over 10 ns. The plot is for one of the two leaflets in the system with POPC:PSMCHOL=2:1:1.

much more pronounced in the non-raft membrane than the raft membranes, as indicated by Figure 5.2.

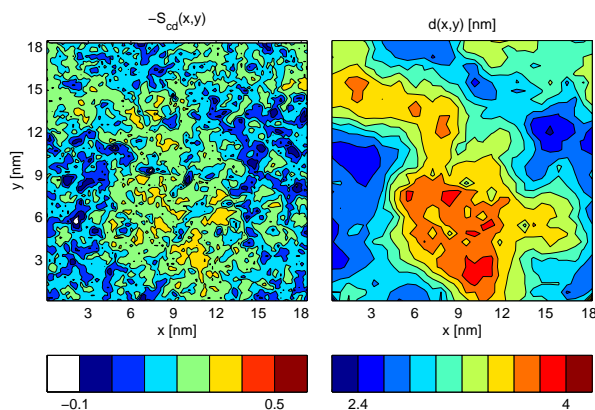


Figure 5.4: The deuterium order parameters of selected carbons (C5-C7) in POPC and PSM chains (left) and the average thickness of the bilayer (right), binned in the xy -plane and averaged over 10 ns. The plot is for one of the two leaflets in the system with POPC:PSMCHOL=62:1:1.

The above conclusions on lateral heterogeneity may be debated because of the slow dynamics and the inadequate conformational sampling in the raft simulations. However, while the two raft-systems were started from different initial configurations, they lead to similar conclusions. Furthermore, a characterisation of the pair distribution functions between the lipids in time display significant changes and convergence over time, which is an indication of relaxation of the structure at small length scales.

5.6 Lateral Pressure Profiles

Figure 5.5 shows the lateral pressure profiles of different kinds of lipid bilayers calculated from MD simulations. It is interesting to note that even though the integral over $\Omega(z)$ must be zero due to the boundary condition $\gamma = 0$, the local pressures within the bilayer are relatively large in magnitude, in the order of 1000 bar. The origins and the nature of the different peaks in $\Omega(z)$ have been discussed in recent literature and for example the pressure has been divided to different force field contributions [Lindahl and Edholm, 2000b; Patra, 2005; Sonne et al., 2005; Ollila, 2006]. In this work, a particular difficulty arises from the relatively large undulations in system S_C , the largest bilayer in fluid phase. To properly gauge the lateral pressure, one should measure the lateral pressure along the contour of the membrane. To simplify the situation, we have limited our discussion either to smaller systems or for the raft-simulations with high k_c , due to suppressed undulations in both.

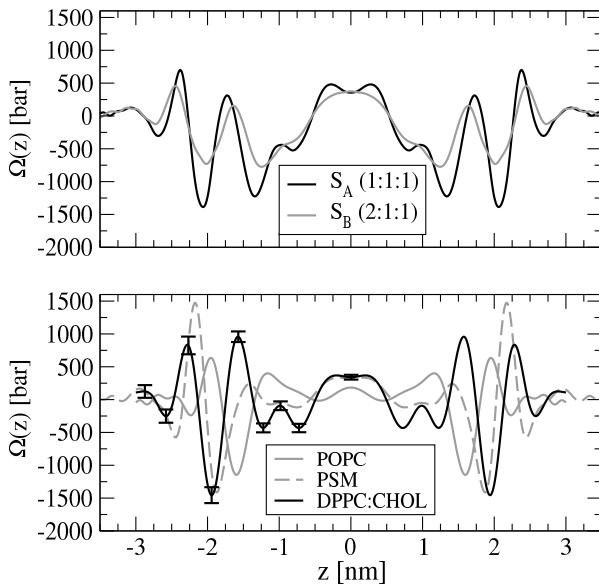


Figure 5.5: Lateral pressure profiles of systems S_A and S_B (top), together with the previously simulated pure POPC/PSM systems and a binary DPPC-CHOL system (bottom). The centre of the membrane is at $z = 0$.

The pressure profiles for different systems, as shown in Figure 5.5 are qualitatively different. In particular, membranes that contain cholesterol display a higher number of peaks when compared to single component bilayers. Also, the raft simulations display further characteristics due to the simultaneous presence of SM and CHOL. Rather than conducting a detailed analysis of all peaks and their origins, we concentrate in the next sections on a more general discussion about possible biological implications and effects on membrane proteins.

5.7 Effects on Membrane Proteins

The possible effects of the above presented results on membrane proteins are manifold. The idea that general physical and elastic properties of the membrane could regulate the partition and activity of membrane proteins has been discussed for example in relation with unsaturated lipids [Ollila et al., 2007], lipid rafts [Simons and Ikonen, 1997] and the mechanism of general anaesthesia [Cantor, 1997, 1998; van den Brink-van der Laan et al., 2004]. However, for some proteins such as the cytochrome bc_1 complex [Palsdottir and Hunte, 2004], specific lipid-protein interactions have been proposed to be important, and indeed, different lipids have varying binding affinities for certain proteins [Powl et al., 2005]. However, a complete picture is probably a combination of the two effects, the specific interactions and the effects from the overall membrane environment. Here, we review the effects related to the latter.

First, the thickness of membranes may be relevant due to the effect of hydrophobic matching [Jensen and Mouritsen, 2004; McIntosh and Simon, 2006]. A good example is the transmembrane protein OmpA, whose free energy of unfolding was reported to change by about $5 k_B T / \text{nm}$ when the hydrophobic thickness of the surrounding saturated PC-membrane was varied [Hong and Tamm, 2004]. Using this value as a simplistic estimate for the effect of hydrophobic thickness, one gets a difference of about $4 k_B T$ in the free energy of unfolding when this particular protein would be transferred from non-raft to raft membrane.

The role of membrane elasticity for protein functionality is emphasised by recent experimental studies, which show that it costs much more energy to deform a membrane by changing its area per lipid than by bending or chain tilting [Kuzmin et al., 2005]. It has been suggested that the free energy to create a protein shaped cavity in a bilayer is proportional to the area compressibility modulus K_A [Zhelev, 1998] and evidence exists that the binding free energy of certain amphipathic peptides indeed depends linearly on K_A [Allende and McIntosh, 2003]. Within this picture, as our data suggests a 5- to 14-fold difference in the values of K_A between raft and non-raft membranes, this practically means a cost in free energy of about 4 to $8 k_B T$ when a membrane protein (Melittin) is transferred from non-raft to raft environment [Allende and McIntosh, 2003].

Another interesting idea relates the bending rigidity of the membrane to the diffusion rates of membrane proteins [Brown, 2003]. The point here is that the cytoskeleton hinders the diffusion of membrane bound proteins, for example in organisms such as fibroblasts, nerve cells, and red blood

cells [Sako and Kusumi, 1995; Winkler et al., 1999; Lin and Brown, 2004]. Brown et al. propose that thermal undulations of the membrane would allow the proteins to escape the confined areas more easily [Brown, 2003]. This relates the undulation amplitudes and the bending rigidity of the membrane directly to the large-scale diffusion coefficient of the membrane proteins. For lipid raft systems with lateral heterogeneity, the slower diffusion within the rafts leads to anomalous diffusion [Nicolau et al., 2007]. The increase of bending rigidity due to the raft domains would impose an additional effect on diffusion, through the interactions with the cytoskeleton.

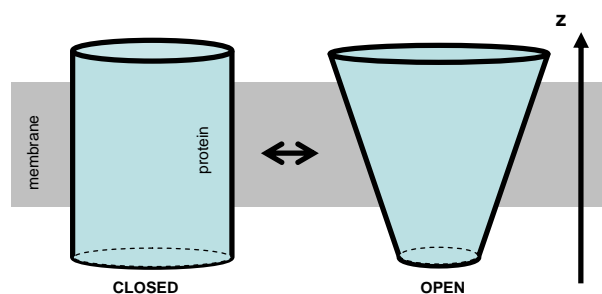


Figure 5.6: Schematic illustration of the two conformations of the membrane protein MscL embedded in a lipid bilayer.

To estimate the effect of pressure profile on membrane proteins one can follow the approach introduced by Cantor [Cantor, 1999] and later also used by Gullingsrud et. al [Gullingsrud and Schulten, 2004]. The idea is to calculate the work ΔW done against the lateral pressure profile when altering the shape of the membrane cavity occupied by the protein as it changes conformation from the closed to an open state. Assuming that the cross-sectional area of the protein changes by ΔA , the work can be written as:

$$\Delta W = \int dz \Omega(z) \Delta A(z). \quad (5.9)$$

As a simple model we use the ion channel MscL, whose conformation changes anisotropically between cylindrical (open) and cone (closed) shapes [Sukharev et al., 2001], see Figure 5.6 for schematic illustration. Both conformations can roughly be described by the cross sectional area of a truncated cone $A(z) = \pi(R + sz)^2$. For the cylindrical case, we have $s = 0$ and $R = 2.5$ nm, and for the closed shape we use the slope of $s = 0.2$ and the origin $z = 0$ with $A(0) = \pi R^2$. The values for s and R are fitted to the experimental structure of MscL and are identical to those used by Gullingsrud et al. [Gullingsrud and Schulten, 2004]. Using this simple scheme, we get

the work against the lateral pressure profile in opening the channel:

$$\Delta W = W_{open} - W_{closed} = \pi \int dz \Omega(z) [R + sz]^2, \quad (5.10)$$

which relates a positive value of ΔW to a lowered open state energy (increased probability) relative to the closed state. Here, one should note that ΔW depends on the second moment of the lateral pressure profile [Gullingsrud and Schulten, 2004] and that it is susceptible to small changes of lateral pressure in particular far from the bilayer centre. In our approach, we calculate the error-bars for ΔW by considering the two monolayers in each system separately.

The integration over the lateral pressure profiles in Figure 5.5 results in $\Delta W = (11 \pm 2)k_B T$ and $(4 \pm 1)k_B T$ for the two raft systems, S_A and S_B in respective order. These are significantly higher than the values found for the pure POPC bilayer $(1.9 \pm 0.2)k_B T$, the pure PSM bilayer $(1.0 \pm 0.6)k_B T$, or the binary DPPC-CHOL bilayer $(1.0 \pm 0.4)k_B T$. The numbers above suggest that the equilibrium probability of MscL to be in open state is significantly altered by the pressure profile and is higher in the raft environment than in the different non-raft environments. As the free energy difference between the open and closed states of MscL has been estimated to be about 20–50 $k_B T$ [Sukharev et al., 1999; Gullingsrud and Schulten, 2004], the pressure profile contributes a significant fraction of this total free energy difference.

CHAPTER 6

Summary

The complexity of biological membranes and the large variety of involved length and timescales calls for the utilisation of different kind of research approaches, involving atom-scale simulations. This study has concentrated on molecular dynamics simulations of lipid bilayers comprised of either one of the following components or a mixture of them: PC, SM and sterols.

The results for single-component SM bilayers showed that the intra- and intermolecular hydrogen bonding leads to significant differences in the bilayer properties when compared with PC. For example, packing of the lipids and the ordering of the acyl chains of the lipids is more pronounced in the SM bilayers. Also, the higher degree of saturation and the long nature of the acyl chains in SM were found to alter the structure and dynamics of the bilayers. In particular, the longer chains of SM were found to interdigitate through the bilayer centre, irrespective of the unsaturation level.

The molecular interactions of CHOL with PC and SM lipids were characterised in detail. A difference in the nature of SM-CHOL interaction was observed when compared with the PC-CHOL interaction. However, no direct hydrogen bonding was found between SM and CHOL, but the difference was shown to be related to the interactions between CHOL and water. Additionally, it was shown that CHOL has a better capacity to order the neighbouring acyl chains than any other studied sterol.

The raft-like membranes were shown to be much more rigid, ordered and packed than the non-raft like membranes, and also characterised by slower

dynamics of the lipids. The different properties of the membrane environments were suggested to have significant implications for membrane proteins, in particular through differences in the lateral pressure profiles of the membrane. As many cellular processes involve membrane proteins, more detailed knowledge of the interactions between proteins and the membrane environment is called for.

Ideas for further studies arising from the results of this work are manifold. First, simulations of single component bilayers should be continued to further understand the characteristics of different lipid species, and to develop ways to better combine simulations with experiments. Also, work on multi-component systems should be continued as well in order to give more insights into the molecular interactions between different lipid species. In particular, this would help in developing new coarse grained models for the different lipid species, which in turn would allow for studies of many slow processes such as phase transition, domain formation, and lipid flip-flop.

Another aspect for the future is to develop new methods and to study extended systems. For example, non-equilibrium studies could be used to provide insight into the possible biological relevance of the chain interdigitation observed for SM. Also, it would be interesting to develop new setups that more realistically describe real biological membranes. For example, simulations on asymmetric bilayers, or bilayers involving glycolipids are rare but doable. Finally, the task of simulating full transmembrane proteins in different lipid environments would provide more solid proof on the features of lipid-protein interactions suggested in this thesis. The task is difficult, but possible in the near future.

Bibliography

- Ågren, J., Muje, P., Hänninen, O., Herranen, J., and Penttilä, I. (1987). Seasonal variations of lipid fatty acids of boreal freshwater fish species. *Comp. Biochem. Physiol.*, 88B:905–909.
- Alder, B. J. and Wainwright, T. E. (1959). Studies in molecular dynamics. I. General method. *J. Chem. Phys.*, 31:459–466.
- Allen, M. P. and Tildesley, D. J. (1990). *Computer Simulation of Liquids*. Oxford University Press, New York.
- Allende, D. and McIntosh, T. J. (2003). Melittin-induced bilayer leakage depends on lipid material properties: Evidence for toroidal pores. *Biophys. J.*, 88:1828–1837.
- Allender, D. W. and Schick, M. (2006). Phase separation in bilayer lipid membranes: Effects on the inner leaf due to coupling to the outer leaf. *Biophys. J.*, 91:2928–2935.
- Almeida, P. F. F., Pokorny, A., and Hinderliter, A. (2005). Thermodynamics of membrane domains. *Biochim. Biophys. Acta*, 1720:1–13.
- Almeida, P. F. F., Vaz, W. L. C., and Thompson, T. E. (1992). Lateral diffusion in the liquid phases of dimyristoylphosphatidylcholine/cholesterol lipid bilayers: A free volume analysis. *Biochemistry*, 31:6739–6747.
- Andersen, O. S. and Koeppe, R. E. (2007). Bilayer thickness and membrane protein function: An energetic perspective. *Annu. Rev. Biophys. Biomol. Struct.*, 36:107–130.
- Anézo, C., de Vries, A. H., Höltje, H.-D., Tieleman, D. P., and Marrink, S.-J. (2003). Methodological issues in lipid bilayer simulations. *J. Phys. Chem. B*, 107:9424–9433.
- Ayton, G. and Voth, G. A. (2002). Bridging microscopic and mesoscopic simulations of lipid bilayers. *Biophys. J.*, 83:3357–3370.
- Bachar, M., Brunelle, P., Tieleman, D. P., and Rauk, A. (2004). Molecular dynamics simulation of a polyunsaturated lipid bilayer susceptible to lipid peroxidation. *J. Phys. Chem. B*, 108:7170–7179.
- Bagatolli, L. A. (2006). To see or not to see: Lateral organization of biological membranes and fluorescence microscopy. *Biochim. Biophys. Acta*,

- 1758:1541–1556.
- Bar, L. K., Barenholz, Y., and Thompson, T. E. (1997). Effect of sphingomyelin composition on the phase structure of phosphatidylcholine-sphingomyelin bilayers. *Biochemistry*, 36:2507–2516.
- Ben-Shaul, A. (1995). Molecular theory of chain packing, elasticity and lipid-protein interaction in lipid bilayers. In Lipowsky, R. and Sackmann, E., editors, *Structure and dynamics of membranes: From cells to vesicles*, pages 359–401. Elsevier, Amsterdam.
- Benz, R. W., Castro-Roman, R., Tobias, D. J., and White, S. H. (2005). Experimental validation of molecular dynamics simulations of lipid bilayers: A new approach. *Biophys. J.*, 88:805–817.
- Berendsen, H. J. C., Postma, J. P. M., van Gunsteren, W. F., DiNola, A., and Haak, J. R. (1984). Molecular dynamics with coupling to an external bath. *J. Chem. Phys.*, 81:3684–3690.
- Berger, O., Edholm, O., and Jähnig, F. (1997). Molecular dynamics simulations of a fluid bilayer of dipalmitoylphosphatidylcholine at full hydration, constant pressure, and constant temperature. *Biophys. J.*, 72:2002–2013.
- Bezrukov, S. M. (2000). Functional consequences of lipid packing stress. *Curr. Opin. Coll. Int. Sci.*, 5:237–243.
- Bloom, M., Evans, E., and Mouritsen, O. G. (1991). Physical properties of the fluid lipid-bilayer component of cell membranes: A perspective. *Q. Rev. Biophys.*, 24:293–397.
- Böckmann, R. A., Hac, A., Heimburg, T., and Grubmüller, H. (2003). Effect of sodium chloride on a lipid bilayer. *Biophys. J.*, 85:1647–1655.
- Brooks, B. R., Bruccoleri, R. E., Olafson, B. D., States, D. J., Swaminathan, S., and Karplus, M. (1983). Charmm: A program for macromolecular energy, minimization, and dynamics calculations. *J. Comp. Chem.*, 4:187–217.
- Brown, F. L. H. (2003). Regulation of protein mobility via thermal membrane undulations. *Biophys. J.*, 84:842–853.
- Brown, R. E. (1998). Sphingolipid organization in biomembranes: What physical studies of model membranes reveal. *J. Cell Sci.*, 111:1–9.
- Cantor, R. S. (1997). The lateral pressure profile in membranes: A physical mechanism of general anesthesia. *Biochemistry*, 36:2339–2344.
- Cantor, R. S. (1998). The lateral pressure profile in membranes: A physical mechanism of general anesthesia. *Toxicol. Lett.*, 100–101:451–458.
- Cantor, R. S. (1999). The influence of membrane lateral pressure on simple geometric models of protein conformational equilibria. *Chem. Phys. Lipids*, 101:45–56.
- Cascales, J. J. L., Ottero, T. F., Smith, B. D., Conzáles, C., and Márquez, M. (2006). Model of an asymmetric DPPC/DPPS membrane: Effect of asymmetry on the lipid properties. A molecular dynamics simulation study. *J. Phys. Chem. B*, 110:2358–2363.
- Chiu, S.-W., Clark, M., Balaji, V., Subramaniam, S., Scott, H. L., and Jakobsson, E. (1995). Incorporation of surface tension into molecular dynamics simulation of an interface: A fluid phase lipid bilayer membrane.

- Biophys. J.*, 69:1230–1245.
- Chiu, S. W., Vasudevan, S., Jakobsson, E., Mashl, R. J., and Scott, H. L. (2003). Structure of sphingomyelin bilayers: A simulation study. *Biophys. J.*, 85:3624–3635.
- Clarke, J. A., Heron, A. J., Seddon, J. M., and Law, R. W. (2006). The diversity of the liquid ordered (lo) phase of phosphatidylcholine/cholesterol membranes: A variable temperature multinuclear solid-state NMR and X-Ray diffraction study. *Biophys. J.*, 90:2383–2393.
- Cordomí, A., Edholm, O., and Perez, J. J. (2007). Effect of different treatments of long-range interactions and sampling conditions in molecular dynamic simulations of rhodopsin embedded in a dipalmitoyl phosphatidylcholine bilayer. *J. Comp. Chem.*, 28:1017–1030.
- Cornell, W. D., Cieplak, P., Bayly, C. I., Gould, I. R., Merz, K. M., Ferguson, D. M., Spellmeyer, D. C., Fox, T., Caldwell, J. W., and Kollman, P. A. (1995). A second generation force field for the simulation of proteins, nucleic acids, and organic molecules. *J. Am. Chem. Soc.*, 117:5179–5197.
- Cottingham, K. (2004). Do you believe in lipid rafts? *Anal. Chem.*, 76:403–406.
- Cournia, Z., Ullmann, G. M., and Smith, J. C. (2007). Differential effects of cholesterol, ergosterol and lanosterol on dipalmitoyl phosphatidylcholine membrane: A molecular dynamics simulation study. *J. Phys. Chem. B*, 111:1786–1801.
- Čurdová, J., Čapcová, P., Plášek, J., Repáková, J., and Vattulainen, I. (2007). Free pyrene probes in gel and fluid membranes: Perspective through atomistic simulations. *J. Phys. Chem. B*, 111:3640–3650.
- Cuvillier, O. (2002). Sphingosine in apoptosis signalling. *Biochim. Biophys. Acta*, 1585:153–162.
- Czub, J. and Baginski, M. (2006). Comparative molecular dynamics study of lipid membranes containing cholesterol and ergosterol. *Biophys. J.*, 90:2368–2382.
- Darden, T., York, D., and Pedersen, L. (1993). Particle Mesh Ewald: An N-log(N) method for Ewald sums in large systems. *J. Chem. Phys.*, 98:10089–10092.
- de Almeida, R. F. M., Loura, L. M. S., Fedorov, A., and Prieto, M. (2005). Lipid rafts have different sizes depending on membrane composition: A time-resolved fluorescence resonance energy transfer study. *J. Mol. Biol.*, 346:1109–1120.
- de Vries, A. H., Chandrasekhar, I., van Gunsteren, W. F., and Hünenberger, P. H. (2005). Molecular dynamics simulations of phospholipid bilayers: Influence of artificial periodicity, system size, and simulation time. *J. Phys. Chem. B.*, 109:11643–11625.
- Devaux, P. F. and Morris, R. (2004). Transmembrane asymmetry and lateral domains in biological membranes. *Traffic*, 5:241–246.
- Edidin, M. (2003a). Lipids on the frontier: A century of cell-membrane bilayers. *Nat. Rev. Mol. Cell. Biol.*, 4:414–416.
- Edidin, M. (2003b). The state of lipid rafts: From model membranes to

- cells. *Annu. Rev. Biophys. Biomol. Struct.*, 32:257–283.
- Egberts, E., Marrink, S.-J., and Berendsen, H. J. C. (1994). Molecular dynamics simulation of a phospholipid membrane. *Eur. Biophys. J.*, 22:423–436.
- Epand, R. M. (2003). Cholesterol in bilayers of sphingomyelin or dihydrosphingomyelin at concentrations found in ocular lens membranes. *Biophys. J.*, 84:3102–3110.
- Epand, R. M. (2004). Do proteins facilitate the formation of cholesterol-rich domains? *Biochim. Biophys. Acta*, 1666:227–238.
- Essex, J. W., Hann, M. M., and Richards, W. G. (1994). Molecular dynamics simulation of a hydrated phospholipid bilayer. *Phil. Trans. R. Soc. Lond. B*, 344:239–260.
- Essmann, U., Perera, L., Berkowitz, M. L., Darden, T., Lee, H., and Pedersen, L. G. (1995). A smooth particle mesh Ewald potential. *J. Chem. Phys.*, 103:8577–8592.
- Evans, E. and Rawicz, W. (1990). Entropy driven tension and bending elasticity in condensed-fluid membranes. *Phys. Rev. Lett.*, 64:2094–2097.
- Ewald, P. P. (1921). Die berechnung optischer und elektrostatischer gitterpotentiale. *Ann. Phys.*, 64:253–287.
- Falck, E., Patra, M., Karttunen, M., Hyvönen, M. T., and Vattulainen, I. (2004). Lessons of slicing membranes: Interplay of packing, free area, and lateral diffusion in phospholipid / cholesterol bilayers. *Biophys. J.*, 87:1076–1091.
- Faller, R. and Marrink, S.-J. (2004). Simulation of domain formation in DLPC-DSPC bilayers. *Langmuir*, 20:7686–7693.
- Feenstra, K. A., Hess, B., and Berendsen, H. J. C. (1999). Improving efficiency of large time-scale molecular dynamics simulations of hydrogen-rich systems. *J. Comp. Chem.*, 20:786–798.
- Feigenson, G. W. (2007). Phase boundaries in biological membranes. *Annu. Rev. Biophys. Biomol. Struct.*, in press.
- Feller, S. E., Gawrisch, K., and MacKerell, A. D. (2002). Polyunsaturated fatty acids in lipid bilayers: Intrinsic environmental contributions to their unique physical properties. *J. Am. Chem. Soc.*, 124:318–326.
- Feller, S. E. and Pastor, R. W. (1996). On simulating lipid bilayers with applied surface tension: Periodic boundary conditions and undulations. *Biophys. J.*, 71:1350–1355.
- Filippov, A., Orädd, G., and Lindblom, G. (2006). Sphingomyelin structure influences the lateral diffusion and raft formation in lipid bilayers. *Biophys. J.*, 90:2086–2092.
- Frenkel, D. and Smit, B. (2002). *Understanding Molecular Simulation: From Algorithms to Applications*. Academic Press, San Diego, 2nd edition.
- Fujiwara, T., Ritchie, K., Murakoshi, H., Jacobson, K., and Kusumi, A. (2002). Phospholipids undergo hop diffusion in compartmentalized cell membrane. *J. Cell Biol.*, 157:1071–1081.
- Futerman, A. H. and Riezman, H. (2005). The ins and outs of sphingolipid synthesis. *Trends Cell Biol.*, 15:312–318.

- Gao, L., Shillcock, J., and Lipowsky, R. (2007). Improved dissipative particle dynamics simulations of lipid bilayers. *J. Chem. Phys.*, 126:015101.
- Gaus, K., Gratton, E., Kable, E. P. W., Jones, A. S., Gelissen, I., Kritharides, L., and Jessup, W. (2003). Visualizing lipid structure and raft domains in living cells with two-photon microscopy. *Proc. Natl. Acad. Sci. USA*, 100:15554–15559.
- Gullingsrud, J. and Schulten, K. (2004). Lipid bilayer pressure profiles and mechanosensitive channel gating. *Biophys. J.*, 86:3496–3509.
- Guo, W., Kurze, V., Huber, T., Afdhal, N. H., Beyer, K., and Hamilton, J. A. (2002). A solid-state NMR study of phospholipid-cholesterol interactions: Sphingomyelin-cholesterol binary systems. *Biophys. J.*, 83:1465–1478.
- Gurtovenko, A. A. and Vattulainen, I. (2007). Lipid transmembrane asymmetry and intrinsic membrane potential: Two sides of the same coin. *J. Am. Chem. Soc.*, in press.
- Haines, T. H. (2001). Do sterols reduce proton and sodium leaks through lipid bilayers. *Progr. Lipid Res.*, 40:299–324.
- Halling, K. K. and Slotte, J. P. (2004). Membrane properties of plant sterols in phospholipid bilayers as determined by differential scanning calorimetry, resonance energy transfer and detergent-induced solubilization. *Biochim. Biophys. Acta*, 1664:161–171.
- Hanada, K. (2006). Discovery of the molecular machinery CERT for endoplasmic reticulum-to-Golgi trafficking of ceramide. *Mol. Cell. Biochem.*, 286:23–31.
- Hancock, J. F. (2006). Lipid rafts: Continuous only from simplistic standpoints. *Nat. Rev. Mol. Cell. Biol.*, 7:456–462.
- Helms, J. B. and Zurzolo, C. (2004). Lipids as targeting signals: Lipid rafts and intracellular trafficking. *Traffic*, 5:247–254.
- Heringdorf, D. M., Himmel, H. M., and Jakobs, K. H. (2002). Sphingosylphosphorylcholine – biological functions and mechanism of action. *Biochim. Biophys. Acta*, 1582:178–189.
- Hess, B., Bekker, H., Berendsen, H. J. C., and Fraaije, J. G. E. M. (1997). LINCS: A linear constraint solver for molecular simulations. *J. Comput. Chem.*, 18:1463–1472.
- Hifeda, Y. F. and Rayfield, G. W. (1992). Evidence for first-order phase transitions in lipid and fatty acid monolayers. *Langmuir*, 8:197–200.
- Hockney, R. W. and Eastwood, J. W. (1988). *Computer simulation using particles*. IOP Publishing, Philadelphia.
- Hofsäss, C., Lindahl, E., and Edholm, O. (2003). Molecular dynamics simulations of phospholipid bilayers with cholesterol. *Biophys. J.*, 84:2192–2206.
- Högberg, C.-J. and Lyubartsev, A. P. (2006). A molecular dynamics investigation of the influence of hydration and temperature on structural and dynamical properties of a dimyristoylphosphatidylcholine bilayer. *J. Phys. Chem. B*, 110:14326–14336.
- Holian, B. L., Voter, A. F., and Ravelo, R. (1995). Thermostatted molec-

- ular dynamics: How to avoid the Toda demon hidden in Nosé-Hoover dynamics. *Phys. Rev. E*, 52:2338–2347.
- Holopainen, J. M., Metso, A. J., Mattila, J.-P., Jutila, A., and Kinnunen, P. K. J. (2004). Evidence for the lack of a specific interaction between cholesterol and sphingomyelin. *Biophys. J.*, 86:1510–1520.
- Höltje, M., Förster, T., Brandt, B., Engels, T., von Rybinski, W., and Höltje, H.-D. (2001). Molecular dynamics simulations of stratum corneum lipid models: Fatty acids and cholesterol. *Biochim. Biophys. Acta*, 1511:156–167.
- Hong, H. and Tamm, L. K. (2004). Elastic coupling of integral membrane protein stability to lipid bilayer forces. *Proc. Natl. Acad. Sci.*, 101:4065–4070.
- Hoover, W. G. (1985). Canonical dynamics: Equilibrium phase-space distributions. *Phys. Rev. A*, 31:1695–1697.
- Hsueh, Y.-W., Chen, M.-T., Patty, P. J., Code, C., Cheng, J., Frisken, B. J., Zuckermann, M., and Thewalt, J. (2007). Ergosterol in POPC membranes: Physical properties and comparison with structurally similar sterols. *Biophys. J.*, 92:1606–1615.
- Huang, J. and Feigenson, G. W. (1999). A microscopic interaction model of maximum solubility of cholesterol in lipid bilayers. *Biophys. J.*, 76:2142–2157.
- Huster, D., Scheidt, H. A., Arnold, K., Herrmann, A., and Müller, P. (2005). Desmosterol may replace cholesterol in lipid membranes. *Biophys. J.*, 88:1838–1844.
- Huwiler, A., Kolter, T., Pfeilschifter, J., and Sandhoff, K. (2000). Physiology and pathophysiology of sphingolipid metabolism and signaling. *Biochim. Biophys. Acta*, 1485:63–99.
- Hyvönen, M. T. and Kovanen, P. T. (2003). Molecular dynamics simulation of sphingomyelin bilayer. *J. Phys. Chem. B*, 107:9102–9108.
- Ibragimova, G. T. and Wade, R. C. (1998). Importance of explicit salt ions for protein stability in molecular dynamics simulation. *Biophys. J.*, 74:2906–2911.
- Ipsen, J. H., Karlström, K., Mouritsen, O. G., Wennerström, H., and Zuckermann, M. J. (1987). Phase equilibria in the phosphatidylcholine-cholesterol system. *Biochim. Biophys. Acta*, 905:162–172.
- Irving, J. H. and Kirkwood, J. G. (1950). The statistical mechanical theory of transport processes. IV. The equations of hydrodynamics. *J. Chem. Phys.*, 18:817–829.
- Israelachvili, J. N. (1985). *Intermolecular and Surface Forces*. Academic Press, Orlando.
- Ito, T. and Tanikawa, K. (2002). Long-term integrators and stability of planetary orbits in our solar system. *Mon. Not. R. Astron. Soc.*, 336:483–500.
- Jacobson, K., Mouritsen, O. G., and Anderson, G. W. (2007). Lipid rafts: At a crossroad between cell biology and physics. *Nat. Cell. Biol.*, 9:7–14.
- Jedlovsky, P. and Mezei, M. (2003). Effect of cholesterol on the properties

- of phospholipid membranes. 2. Free energy profile of small molecules. *J. Phys. Chem. B*, 107:5322–5332.
- Jensen, M. O. and Mouritsen, O. G. (2004). Lipids do influence protein function: The hydrophobic – matching hypothesis revisited. *Biochim. Biophys. Acta*, 1666:205–226.
- Jönsson, B., Edholm, O., and Teleman, O. (1986). Molecular dynamics simulations of a sodium octanoate micelle in aqueous solution. *J. Chem. Phys.*, 85:2259–2271.
- Jorgensen, W. L. and Tirado-Rives, J. (1988). The OPLS potential functions for proteins. Energy minimizations for crystals of cyclic peptides and crambin. *J. Am. Chem. Soc.*, 110:1657–1666.
- Khelashvili, G. A. and Scott, H. L. (2004). Combined Monte Carlo and molecular dynamics simulation of hydrated 18:0 sphingomyelin-cholesterol lipid bilayers. *J. Chem. Phys.*, 120:9841–9847.
- Klauda, J. B., Brooks, B. R., and Pastor, R. W. (2006). Dynamical motions of lipids and a finite size effect in simulations of bilayers. *J. Chem. Phys.*, 125:144710.
- Knecht, V., Mark, A. E., and Marrink, S.-J. (2006). Phase behaviour of phospholipid/fatty acid/water mixture studied in atomic detail. *J. Am. Chem. Soc.*, 128:2030–2034.
- König, S., Pfeiffer, W., Bayerl, T., Richter, D., and Sackmann, E. (1992). Molecular dynamics of lipid bilayers studied by incoherent quasi-elastic neutron scattering. *J. Phys. II France*, 2:1589–1615.
- Korstanje, L. J., van Ginkel, G., and Levine, Y. K. (1990). Effects of steroid molecules on the dynamical structure of dioleoylphosphatidylcholine and digalactosyldiacylglycerol bilayers. *Biochim. Biophys. Acta*, 1022:155–162.
- Kox, A. J., Michels, J. P. J., and Wiegel, F. W. (1980). Simulation of a lipid monolayer using molecular dynamics. *Nature*, 287:317–319.
- Koynova, R. and Caffrey, M. (1995). Phases and phase transitions of the sphingolipids. *Biochim. Biophys. Acta*, 1255:213–236.
- Koynova, R. and Caffrey, M. (1998). Phases and phase transitions of the phosphatidylcholines. *Biochim. Biophys. Acta*, 1376:91–145.
- Kučerka, N., Tristram-Nagle, S., and Nagle, J. F. (2005). Structure of fully hydrated fluid phase lipid bilayers with monounsaturated chains. *J. Membrane Biol.*, 208:193–202.
- Kučerka, N., Tristram-Nagle, S., and Nagle, J. F. (2006). Closer look at structure of fully hydrated fluid phase DPPC bilayers. *Biophys. J.*, 90:L83–L85.
- Kupiainen, M., Falck, E., Ollila, S., Niemelä, P., Gurtovenko, A. A., Hyvönen, M. T., Patra, M., Karttunen, M., and Vattulainen, I. (2005). Free volume properties of sphingomyelin, DMPC, DPPC, and PLPC bilayers. *J. Comput. Theor. Nanosci.*, 2:401–413.
- Kuzmin, P. I., Akimov, S. A., Chizmadzhev, Y. A., Zimmerberg, J., and Cohen, F. S. (2005). Line tension and interaction energies of membrane rafts calculated from lipid splay and tilt. *Biophys. J.*, 88:1120–1133.
- Ladanyi, B. M. and Skaf, M. S. (1993). Computer simulation of hydrogen-

- bonding liquids. *Annu. Rev. Phys. Chem.*, 44:335–368.
- Leekumjorn, S. and Sum, A. K. (2007). Molecular studies of the gel to liquid-crystalline phase transition for fully hydrated DPPC and DPPE bilayers. *Biochim. Biophys. Acta.*, 1768:354–365.
- Levitt, M. and Lifson, S. (1969). Refinement of protein conformations using a macromolecular energy minimization procedure. *J. Mol. Biol.*, 46:269–279.
- Li, X.-M., Momsen, M. M., Smaby, J. M., Brockman, H. L., and Brown, R. E. (2001). Cholesterol decreases the interfacial elasticity and detergent solubility of sphingomyelins. *Biochemistry*, 40:5954–5963.
- Li, X.-M., Smaby, J. M., Momsen, M. M., Brockman, H. L., and Brown, R. E. (2000). Sphingomyelin interfacial behavior: The impact of changing acyl chain composition. *Biophys. J.*, 78:1921–1931.
- Lifson, S. and Warshel, A. (1968). Consistent force field for calculations of conformations, vibrational spectra, and enthalpies of cycloalkane and *n*-alkane molecules. *J. Chem. Physics.*, 49:5116–5129.
- Lin, L. C.-L. and Brown, F. L. H. (2004). Dynamics of pinned membranes with application to protein diffusion on the surface of red blood cells. *Biophys. J.*, 86:764–780.
- Lindahl, E. and Edholm, O. (2000a). Mesoscopic undulations and thickness fluctuations in lipid bilayers from molecular dynamics simulations. *Biophys. J.*, 79:426–433.
- Lindahl, E. and Edholm, O. (2000b). Spatial and energetic-entropic decomposition of surface tension in lipid bilayers from molecular dynamics simulations. *J. Chem. Phys.*, 113:3882–3893.
- Lindahl, E. and Edholm, O. (2001). Molecular dynamics simulation of NMR relaxation rates and slow dynamics in lipid bilayers. *J. Chem. Phys.*, 115:4938–4950.
- London, E. (2005). How principles of domain formation in model membranes may explain ambiguities concerning lipid raft formation in cells. *Biochim. Biophys. Acta*, 1746:203–220.
- Luzar, A. and Chandler, D. (1996). Effect of environment on hydrogen bond dynamics in liquid water. *Phys. Rev. Lett.*, 76:928–931.
- MacKerell, A. D. (2004). Empirical force fields for biological macromolecules: Overview and issues. *J. Comput. Chem.*, 25:1584–1604.
- MacKerell, A. D., Bashford, D., Bellott, M., Dunbrack, R. L., Evanseck, J. D., Field, J., Fischer, S., Gao, J., Guo, H., Ha, S., Joseph-McCarthy, D., Kuchnir, L., Kuczera, K., Lau, F. T. K., Mattos, C., Michnick, S., Ngo, T., Nguyen, D. T., Prodhom, B., Reiher, W. E., Roux, B., Schlenkrich, M., Smith, J. C., Stote, R., Straub, J., Watanabe, M., Wiorkiewicz-Kuczera, J., Yin, D., and Karplus, M. (1998). All-atom empirical potential for molecular modeling and dynamics studies of proteins. *J. Phys. Chem. B*, 102:3586–3616.
- Marrink, S.-J., de Vries, A. H., and Mark, A. E. (2004). Coarse grained model for semiquantitative lipid simulations. *J. Phys. Chem. B*, 108:750–760.

- Marrink, S.-J. and Mark, A. E. (2004). Molecular view of hexagonal phase formation in phospholipid membranes. *Biophys. J.*, 87:3894–3900.
- Marrink, S. J., Risselada, J., and Mark, A. E. (2005). Simulation of gel phase formation and melting in lipid bilayers using a coarse grained model. *Chem. Phys. Lipids*, 135:223–244.
- Marsh, D. (1991). General features of phospholipid phase transitions. *Chem. Phys. Lipids*, 57:109–120.
- Marsh, D. (1997). Renormalization of the tension and area expansion modulus in fluid membranes. *Biophys. J.*, 73:865–869.
- Mashl, R. J., Scott, H. L., Subramaniam, S., and Jakobsson, E. (2001). Molecular simulation of dioleoylphosphatidylcholine lipid bilayers at differing levels of hydration. *Biophys. J.*, 81:3005–3015.
- Mason, R. P., Tulenko, T. N., and Jacob, R. F. (2003). Direct evidence for cholesterol crystalline domains in biological membranes: Role in human pathobiology. *Biochim. Biophys. Acta*, 1610:198–207.
- Maulik, P. R., Atkinson, D., and Shipley, G. G. (1986). X-ray scattering of vesicles of *N*-acyl sphingomyelins: Determination of bilayer thickness. *Biophys. J.*, 50:1071–1077.
- Maulik, P. R. and Shipley, G. G. (1996). *N*-palmitoyl sphingomyelin bilayers: Structure and interactions with cholesterol and dipalmitoylphosphatidylcholine. *Biochemistry*, 35:8025–8034.
- Maxfield, F. R. (2002). Plasma membrane microdomains. *Curr. Opin. Cell Biol.*, 14:483–487.
- McConnell, H. M. and Vrljic, M. (2003). Liquid-liquid immiscibility in membranes. *Annu. Rev. Biophys. Biomol. Struct.*, 32:469.
- McIntosh, T. J. and Simon, S. A. (2006). Roles of bilayer material properties in function and distribution of membrane properties. *Annu. Rev. Biophys. Biomol. Struct.*, 35:177–198.
- Mehnert, T., Jacob, K., Bittman, R., and Beyer, K. (2006). Structure and lipid interaction of *N*-palmitoylsphingomyelin in bilayer membranes as revealed by 2H-NMR spectroscopy. *Biophys. J.*, 90:939–946.
- Miyamoto, S. and Kollman, P. A. (1992). SETTLE: An analytical version of the SHAKE and RATTLE algorithms for rigid water models. *J. Comput. Chem.*, 13:952–962.
- Mombelli, E., Morris, R., Taylor, W., and Fraternali, F. (2003). Hydrogen-bonding propensities of sphingomyelin in solution and in a bilayer assembly: A molecular dynamics study. *Biophys. J.*, 84:1507–1517.
- Moore, G. E. (1965). Cramming more components onto integrated circuits. *Electronics*, 38(8).
- Mouritsen, O. G. and Jorgensen, K. (1994). Dynamical order and disorder in lipid bilayers. *Chem. Phys. Lipids*, 73:3–25.
- Murtola, T., Falck, E., Patra, M., Karttunen, M., and Vattulainen, I. (2004). Coarse-grained model for phospholipid/cholesterol bilayer. *J. Chem. Phys.*, 121:9156–9165.
- Nagle, J. F. and Tristram-Nagle, S. (2000). Structure of lipid bilayers. *Biochim. Biophys. Acta*, 1469:159–195.

- Needham, D., McIntosh, T. J., and Evans, E. (1988). Thermomechanical and transition properties of dimyristoylphosphatidylcholine/cholesterol bilayers. *Biochemistry*, 27:4668–4673.
- Needham, D. and Nunn, R. S. (1990). Elastic deformation and failure of lipid bilayer membranes containing cholesterol. *Biophys. J.*, 58:997–1009.
- Nelson, D. L. and Cox, M. M. (2005). *Lehninger Principles of Biochemistry*. W. H. Freeman and Company, New York, 4th edition.
- Neuringer, L. J., Sears, B., Jungalwala, F. B., and Shriver, E. K. (1979). Difference in orientational order in phospholipid and sphingomyelin bilayers. *FEBS Lett.*, 104:173–175.
- Nicolau, D. V., Hancock, J. F., and Burrage, K. (2007). Sources of anomalous diffusion on cell membranes: A Monte Carlo study. *Biophys. J.*, 92:1975–1987.
- Nosé, S. (1984). A molecular dynamics method for simulations in the canonical ensemble. *Mol. Phys.*, 52:255–268.
- Nosé, S. and Klein, M. L. (1983). Constant pressure molecular dynamics for molecular systems. *Mol. Phys.*, 50:1055–1076.
- Ohanian, J. and Ohanian, V. (2001). Sphingolipids in mammalian cell signalling. *Cell. Mol. Life Sci.*, 58:2053–2068.
- Ohvo-Rekilä, H., Ramstedt, B., Leppimäki, P., and Slotte, J. P. (2002). Cholesterol interactions with phospholipids in membranes. *Prog. Lipid Res.*, 41:66–97.
- Oldfield, E. and Chapman, D. (1972). Dynamics of lipid membranes: Heterogeneity and the role of cholesterol. *FEBS Lett.*, 23:285–297.
- Ollila, S. (2006). Lateral pressure profile calculations of lipid membranes from atomic scale molecular dynamics simulations. Master's thesis, Helsinki Univ. Tech.
- Ollila, S., Hyvönen, M. T., and Vattulainen, I. (2007). Polyunsaturation in lipid membranes: Dynamic properties and lateral pressure profiles. *J. Phys. Chem. B.*, 111:3139–3150.
- Onsager, L. (1936). Electric moments of molecules in lipids. *J. Am. Chem. Soc.*, 58:1486–1493.
- Orädd, G. and Lindblom, G. (2004). Lateral diffusion studied by pulsed field gradient NMR on oriented lipid membranes. *Magn. Reson. Chem.*, 42:123–131.
- Palsdottir, H. and Hunte, C. (2004). Lipids in membrane protein structures. *Biochim. Biophys. Acta*, 1666:2–18.
- Pandit, S. A., Chiu, S.-W., Jakobsson, E., Grama, A., and Scott, H. L. (2007). Cholesterol surrogates: A comparison of cholesterol and 16:0 ceramide in POPC bilayers. *Biophys. J.*, 92:920–927.
- Pandit, S. A., Jakobsson, E., and Scott, H. L. (2004a). Simulation of the early stages of nano-domain formation in mixed bilayers of sphingomyelin, cholesterol, and dioleoylphosphatidylcholine. *Biophys. J.*, 87:3312–3322.
- Pandit, S. A., Vasudevan, S., Chiu, S. W., Mashl, R. J., Jakobsson, E., and Scott, H. L. (2004b). Sphingomyelin-cholesterol domains in phospholipid membranes: Atomistic simulation. *Biophys. J.*, 87:1092–1100.

- Parrinello, M. and Rahman, A. (1981). Polymorphic transitions in single crystals: A new molecular dynamics method. *J. Appl. Phys.*, 52:7182–7190.
- Pastor, R. W. (1994). Molecular dynamics and Monte Carlo simulations of lipid bilayers. *Curr. Opin. Struct. Biol.*, 4:486–492.
- Pastor, R. W. and Feller, S. E. (1996). Time scales of lipid dynamics and molecular dynamics. In Merz, K. M. and Roux, B., editors, *Biological membranes: A molecular perspective from computation and experiment*, pages 3–30. Birkhauser, Boston.
- Pastor, R. W., Venable, R. M., and Feller, S. E. (2002). Lipid bilayers, NMR relaxation and computer simulations. *Acc. Chem. Res.*, 35:438–446.
- Patel, R. Y. and Balaji, P. V. (2005). Effect of the choice of the pressure coupling method on the spontaneous aggregation of DPPC molecules. *J. Phys. Chem. B*, 109:14667–14674.
- Patra, M., Hyvönen, M. T., Falck, E., Sabouri-Ghomi, M., Vattulainen, I., and Karttunen, M. (2007). Long-range interactions and parallel scalability in molecular simulations. *Comp. Phys. Comm.*, 176:14–22.
- Patra, M. (2005). Lateral pressure profiles in cholesterol-DPPC bilayers. *Eur. Biophys. J.*, 35:79–88.
- Patra, M., Karttunen, M., Hyvönen, M. T., Falck, E., Lindqvist, P., and Vattulainen, I. (2003). Molecular dynamics simulations of lipid bilayers: Major artifacts due to truncating electrostatic interactions. *Biophys. J.*, 84:3636–3645.
- Patra, M., Salonen, E., Terama, E., Vattulainen, I., Faller, R., Lee, B. W., Holopainen, J., and Karttunen, M. (2006). Under the influence of alcohol: The effect of ethanol and methanol on lipid bilayers. *Biophys. J.*, 90:1121–1135.
- Petrache, H. I., Dodd, S. W., and Brown, M. F. (2000). Area per lipid and acyl length distributions in fluid phosphatidylcholines determined by ^2H NMR spectroscopy. *Biophys. J.*, 79:3172–3192.
- Pike, L. J. (2004). Lipid rafts: Heterogeneity on the high seas. *Biochem. J.*, 378:281–292.
- Pike, L. J. (2006). Rafts defined: a report on the keystone symposium on lipid rafts and cell function. *J. Lipid Res.*, 47:1597–1598.
- Pitman, M. C., Suits, F., Gawrisch, K., and Feller, S. E. (2005). Molecular dynamics investigation of dynamical properties of phosphatidylethanoamine lipid bilayers. *J. Chem. Phys.*, 122:244715.
- Pitman, M. C., Suits, F., MacKerell, A. D., and Feller, S. E. (2004). Molecular-level organization of saturated and polyunsaturated fatty acids in a phosphatidylcholine bilayer containing cholesterol. *Biochemistry*, 43:15318–15328.
- Plowman, S. J., Muncke, C., Parton, R. G., and Hancock, J. F. (2005). H-ras, K-ras, and inner plasma membrane raft proteins operate in nanoclusters with differential dependence on the actin cytoskeleton. *Proc. Natl. Acad. Sci.*, 102:15500–15505.
- Ponder, J. B. and Case, D. A. (2003). Force fields for protein simulations.

- Adv. Prot. Chem.*, 66:27–85.
- Powl, A. M., Carney, J., Maurius, P., East, J. M., and Lee, A. G. (2005). Mechanistic and functional studies of proteins. *Biochem. Soc. Trans.*, 33:905–909.
- Purves, W. K., Sadava, D., Orians, G. H., and Heller, H. C. (2004). *Life - The Science of Biology*. Sinauer Associates and W. H. Freeman, U.S.A., 7th edition.
- Qiu-Dong, W. (1991). The global solution of the N-body problem. *Celest. Mech. Dyn. Astr.*, 50:73–88.
- Rahman, A. (1964). Correlations in the motion of atoms in liquid argon. *Phys. Rev.*, 136:A405–A411.
- Ramstedt, B., Leppimäki, P., Axberg, M., and Slotte, J. P. (1999). Analysis of natural and synthetic sphingomyelins using high-performance thin-layer chromatography. *Eur. J. Biochem.*, 266:997–1002.
- Ramstedt, B. and Slotte, J. P. (2002). Membrane properties of sphingomyelins. *FEBS Lett.*, 531:33–37.
- Rawicz, W., Olbrich, K. C., McIntosh, T., Needham, D., and Evans, E. (2000). Effect of chain length and unsaturation on elasticity of lipid bilayers. *Biophys. J.*, 79:328–339.
- Rheinstädter, M. C., Seydel, T., w. Häußler, and Salditt, T. (2006). Exploring the collective dynamics of lipid membranes with inelastic neutron scattering. *J. Vac. Sci. Technol.*, 24:1191–1196.
- Rinia, H. A., Snel, M. M. E., van der Eerden, J. P. J. M., and de Kruijff, B. (2001). Visualizing detergent resistant domains in model membranes with atomic force microscopy. *FEBS Lett.*, 501:92–96.
- Róg, T., Murzyn, K., and Pasenkiewicz-Gierula, M. (2003). Molecular dynamics simulations of charged and neutral lipid bilayers: Treatment of electrostatic interactions. *Acta Biochim. Pol.*, 50:789–798.
- Róg, T. and Pasenkiewicz-Gierula, M. (2006a). Cholesterol effects on a mixed-chain phosphatidylcholine bilayer: A molecular dynamics simulation study. *Biochimie*, 88:449–460.
- Róg, T. and Pasenkiewicz-Gierula, M. (2006b). Cholesterol-sphingomyelin interactions: A molecular dynamics simulation study. *Biophys. J.*, 91:3756–3767.
- Róg, T., Pasenkiewicz-Gierula, M., Vattulainen, I., and Karttunen, M. (2007). What happens if cholesterol is made smoother: Importance of methyl substituents in cholesterol ring structure on phosphatidylcholine-sterol interaction. *Biophys. J.*, in press.
- Róg, T., Vattulainen, I., and Karttunen, M. (2005). Modelling glycolipids: Take one. *Cell. Mol. Biol. Lett.*, 10:625–630.
- Ryckaert, J.-P. and Bellemans, A. (1978). Molecular dynamics of liquid alkanes. *Faraday Disc. Chem. Soc.*, 66:95–106.
- Ryckaert, J.-P., Ciccotti, G., and Berendsen, H. J. C. (1977). Numerical integration of the cartesian equations of motion of a system with constraints: Molecular dynamics of n-alkanes. *J. Comp. Phys.*, 23:327–341.
- Sackmann, E. (1995). Biological membranes architecture and function. In

- Lipowsky, R. and Sackmann, E., editors, *Structure and dynamics of membranes: From cells to vesicles*, pages 1–65. Elsevier, Amsterdam.
- Safran, S. (1994). *Statistical Thermodynamics of Surfaces, Interfaces and Membranes*. Addison-Wesley, New York.
- Sako, Y. and Kusumi, A. (1995). Barriers for lateral diffusion of transferrin receptor in the plasma membrane as characterized by receptor dragging by laser tweezers: Fence versus tether. *J. Cell. Biol.*, 129:1559–1574.
- Salaün, C., James, D. J., and Chamberlain, L. H. (2004). Lipid rafts and the regulation of exocytosis. *Traffic*, 5:255–264.
- Sankaram, M. B. and Thompson, T. E. (1990). Modulation of phospholipid acyl chain order by cholesterol. A solid-state ^2H nuclear magnetic resonance study. *Biochemistry*, 29:10676–10684.
- Schlick, T. (2002). *Molecular Modeling and Simulation: An Interdisciplinary Guide*. Springer Verlag, New York.
- Schuck, S. and Simons, K. (2004). Polarized sorting in epithelial cells: Raft clustering and the biogenesis of the apical membrane. *J. Cell. Sci.*, 117:5955–5964.
- Schuler, I., Milon, A., Nakatani, Y., Ourison, G., Albrecht, A.-M., Benveniste, P., and Hartmann, M.-A. (1991). Differential effects of plant sterols on water permeability and on acyl chain ordering of soybean phosphatidylcholine bilayers. *Proc. Natl. Acad. Sci. USA*, 88:6926–6930.
- Schwille, P., Korlach, J., and Webb, W. W. (1999). Fluorescence correlation spectroscopy with single-molecule sensitivity on cell and model membranes. *Cytometry*, 36:176–182.
- Sciortino, F., Poole, P. H., Stanley, H. E., and Havlin, S. (1990). Lifetime of the bond network and gel-like anomalies in supercooled water. *Phys. Rev. Lett.*, 64:1686–1689.
- Seelig, A. and Seelig, J. (1974). The dynamic structure of fatty acyl chains in a phospholipid bilayer measured by deuterium magnetic resonance. *Biochemistry*, 13:4839–4845.
- Shimshick, E. J. and McConnell, M. (1973). Lateral phase separation in phospholipid membranes. *Biochemistry*, 12:2373–2360.
- Shkulipa, S. A., den Otter, W. K., and Briels, W. J. (2005). Surface viscosity, diffusion, and intermonolayer friction: Simulating sheared amphiphilic bilayers. *Biophys. J.*, 89:823–829.
- Silvius, J. R. (2003). Role of cholesterol in lipid raft formation: Lessons from lipid model systems. *Biochim. Biophys. Acta*, 1610:174–183.
- Siminovitch, D. J. and Jeffrey, K. R. (1981). Orientational order in the choline headgroup of sphingomyelin: A ^{14}N -NMR study. *Biochim. Biophys. Acta*, 645:270–278.
- Simons, K. and Ehehalt, R. (2002). Cholesterol, lipid rafts, and disease. *J. Clin. Invest.*, 110:597–603.
- Simons, K. and Ikonen, E. (1997). Functional rafts in cell membranes. *Nature*, 387:569–572.
- Simons, K. and Ikonen, E. (2000). How cells handle cholesterol. *Science*, 290:1721–1726.

- Simons, K. and Vaz, W. L. C. (2004). Model system, lipid rafts, and cell membranes. *Annu. Rev. Biophys. Biomol. Struct.*, 33:269–295.
- Singer, S. J. and Nicolson, G. L. (1972). The fluid mosaic model of the structure of cell membranes. *Science*, 175:720–731.
- Slotte, J. P. (1999). Sphingomyelin–cholesterol interactions in biological and model membranes. *Chem. Phys. Lipids*, 102:13–27.
- Smith, P. E. and Pettitt, B. M. (1996). Ewald artifacts in liquid state molecular dynamics simulations. *J. Chem. Phys.*, 105:4289–4293.
- Smondryev, A. M. and Berkovitz, M. (2001). Molecular dynamics simulation of the structure of dimyristoylphosphatidylcholine bilayers with cholesterol, ergosterol, and lanosterol. *Biophys. J.*, 80:1649–1658.
- Sonne, J., Hansen, F. Y., and Peters, G. H. (2005). Methodological problems in pressure profile calculations for lipid bilayers. *J. Chem. Phys.*, 122:124903.
- Steinbauer, B., Mehnert, T., and Beyer, K. (2003). Hydration and lateral organization in phospholipid bilayers containing sphingomyelin: A ^2H -NMR study. *Biophys. J.*, 85:1013–1024.
- Sukharev, S., Durell, S. R., and Guy, H. R. (2001). Structural models of the MscL gating mechanism. *Biophys. J.*, 81:917–936.
- Sukharev, S. I., Sigurdson, W. J., Kung, C., and Sachs, F. (1999). Energetic and spatial parameters for gating of the bacterial large conductance mechanosensitive channel, MscL. *J. Gen. Physiol.*, 113:525–593.
- Sun, F. (2002). Constant normal pressure, constant surface tension, and constant temperature molecular dynamics simulation of hydrated 1,2-dilignoceroylphosphatidylcholine monolayer. *Biophys. J.*, 82:2511–2519.
- Tabas, I. (2002). Consequences of cellular cholesterol accumulation: basic concepts and physiological implications. *J. Clin. Invest.*, 110:905–911.
- Talbott, C. M., Vorobyov, I., Borchman, D., Taylor, K. G., DuPré, D. B., and Yappert, M. C. (2000). Conformational studies of sphingolipids by NMR spectroscopy. II. Sphingomyelin. *Biochim. Biophys. Acta*, 1467:326–337.
- Templer, R. H., Castle, S. J., Curran, A. R., Rumbles, G., and Klug, D. R. (1998). Sensing isothermal changes in the lateral pressure in model membranes using di-pyrenyl phosphatidylcholine. *Faraday Discuss.*, 111:41–53.
- Térová, B., Slotte, J. P., and Nyholm, K. M. (2004). Miscibility of acyl-chain defined phosphatidylcholines with N-palmitoyl sphingomyelin in bilayer membranes. *Biochim. Biophys. Acta*, 1667:182–189.
- Thudicum, J. L. W. (1884). In *A Treatise on the Chemical Constitution of the Brain*. London.
- Tieleman, D. P. and Berendsen, H. J. C. (1996). Molecular dynamics simulations of a fully hydrated dipalmitoylphosphatidylcholine bilayer with different macroscopic boundary conditions and parameters. *J. Chem. Phys.*, 105:4871–4880.
- Tieleman, D. P. and Berendsen, H. J. C. (1998). A molecular dynamics study of the pores formed by *escherichia coli* OmpF porin in a fully hydrated palmitoyloleoylphosphatidylcholine bilayer. *Biophys. J.*, 74:2786–2801.

- Tieleman, D. P., MacCallum, J. L., Ash, W. L., Kandt, C., Xu, Z., and Monticelli, L. (2006). Membrane protein simulations with a united-atom lipid and all-atom protein model: Lipid-protein interactions, side chain transfer free energies and model proteins. *J. Phys.: Condens. Matter*, 18:S1221–S1234.
- Tieleman, D. P., Marrink, S. J., and Berendsen, H. J. C. (1997). A computer perspective of membranes: Molecular dynamics studies of lipid bilayer systems. *Biochim. Biophys. Acta*, 1331:235–270.
- Tristram-Nagle, S. and Nagle, J. F. (2004). Lipid bilayers: Thermodynamics, structure, fluctuations, and interactions. *Chem. Phys. Lipids*, 127:3–14.
- Tu, K., Tobias, D. J., Blasie, K., and Klein, M. L. (1996). Molecular dynamics investigation of the structure of a fully hydrated gel-phase dipalmitoylphosphatidylcholine bilayer. *Biophys. J.*, 70:595–608.
- Urbina, J. A., Pekerar, S., Le, H., Patterson, J., Montez, B., and Oldfield, E. (1995). Molecular order and dynamics of phosphatidylcholine bilayer membranes in the presence of cholesterol, ergosterol and lanosterol: A comparative study using ^2H -, ^{13}C - and ^{31}P -NMR spectroscopy. *Biochim. Biophys. Acta*, 1238:163–176.
- Vainio, S., Jansen, M., Koivusalo, M., Róg, T., Karttunen, M., Vattulainen, I., and Ikonen, E. (2006). Significance of sterol structural specificity. Desmosterol cannot replace cholesterol in lipid rafts. *J. Biol. Chem.*, 281:348–355.
- van Buuren, A. R., Marrink, S.-J., and Berendsen, H. J. C. (1993). A molecular dynamics study of the decane/water interface. *J. Phys. Chem.*, 97:9206–9212.
- van den Brink-van der Laan, E., Chupin, V., Killian, J. A., and de Kruijff, B. (2004). Small alcohols destabilize the KcsA tetramer via their effect on the membrane lateral pressure. *Biochemistry*, 43:5937–5942.
- van der Ploeg, P. and Berendsen, H. J. C. (1982). Molecular dynamics simulation of a bilayer membrane. *J. Chem. Phys.*, 76:3271–3276.
- van der Spoel, D., Lindahl, E., Hess, B., van Buuren, A. R., Apol, E., Meulenhoff, P. J., Tieleman, D. P., Sijbers, A. L. T. M., Feenstra, K. A., van Drunen, R., and Berendsen, H. J. C. (2005). *Gromacs User Manual version 3.3*. www.gromacs.org.
- van Gunsteren, W. F. and Berendsen, H. J. C. (1987). *Gromos-87 manual*. Biomos BV, Nijenborgh 4, 9747 AG Groningen, The Netherlands.
- van Gunsteren, W. F., Daura, X., and Mark, A. E. (1998). Gromos force field. In *Encyclopedia of Computational Chemistry*, pages 1211–1216. Wiley.
- van Meer, G. (2005). Cellular lipidomics. *EMBO J.*, 24:3159–3165.
- Varma, R. and Mayor, S. (1998). GPI-anchored proteins are organized in submicron domains at the cell surface. *Nature*, 394:798–801.
- Veiga, M. P., Arrondo, J. L. R., goni, F. M., Alonso, A., and Marsh, D. (2001). Interaction of cholesterol in mixed membranes containing phosphatidylcholine, studied by spin-label ESR and IR spectroscopies. A pos-

- sible stabilization of gel-phase sphingolipid domains by cholesterol. *Biochemistry*, 40:2614–2622.
- Vist, M. R. and Davis, J. H. (1990). Phase equilibria of cholesterol/dipalmitoylphosphatidylcholine mixtures: ^2H nuclear magnetic resonance and differential scanning calorimetry. *Biochemistry*, 29:451–464.
- Wassall, S. R., Brzustowicz, M. R., Shaikh, S. R., Cherezov, V., Caffrey, M., and Stillwell, W. (2004). Order from disorder, coralling cholesterol with chaotic lipids; the role of polyunsaturated lipids in membrane raft formation. *Chem. Phys. Lipids*, 132:79–88.
- Weber, W., Hünenberger, P. H., and McCammon, J. A. (2000). Molecular dynamics simulations of a polyalanine octapeptide under Ewald boundary conditions: Influence of artificial periodicity on peptide conformation. *J. Phys. Chem. B*, 104:3668–3675.
- Weiner, S. J., Kollman, P. A., Case, D. A., Singh, U. C., Ghio, C., Alagona, G., Profeta, S., and Weiner, P. (1984). A new force field for molecular mechanical simulation of nucleic acids and proteins. *J. Am. Chem. Soc.*, 106:765–784.
- Winkler, B., Forscher, P., and Mellman, I. (1999). A diffusion barrier maintains distribution of membrane proteins in polarized neurons. *Nature*, 397:698–701.
- Wohlert, J. and Edholm, O. (2004). The range and shielding of dipole-dipole interactions in phospholipid bilayers. *Biophys. J.*, 87:2433–2445.
- Wohlert, J. and Edholm, O. (2006). Dynamics in atomistic simulations of phospholipid membranes: Nuclear magnetic resonance relaxation rates and lateral diffusion. *J. Chem. Phys.*, 125:204703.
- Xiang, T. (1993). Translational diffusion in lipid bilayers: Dynamic free-volume theory and molecular dynamics simulation. *J. Phys. Chem. B*, 294:1–14.
- Zachowski, A. (1993). Phospholipids in animal eukaryotic membranes: Transverse asymmetry and movement. *Biochem. J.*, 294:1–14.
- Zhelev, D. V. (1998). Material property characteristics for lipid bilayers containing lysolipid. *Biophys. J.*, 75:321–330.
- Zielkiewicz, J. (2005). Structural properties of water: Comparison of the SPC, SPCE, TIP4P, and TIP5P models of water. *J. Chem. Phys.*, 123:104501.